Annual Review
2017

Molecular Photoscience Research Center

Kobe University

Preface

This annual review provides a summary of the research activity of Molecular Photoscience Research Center for the 2017 academic year. We are further promoting advanced research and international collaboration on molecular photoscience and related topics. Any constructive comments and questions, and any suggestion for collaboration research are welcome.

This year we have started joint usage/research project on molecular science in the terahertz frequency region, which is open to domestic universities and research institutes. The project is supported by Ministry of Education, Culture, Sports, Science and Technology (MEXT), Japan. In this year 33 joint research projects were accepted, and the research area spans from solid state physics, biophysics, solution chemistry, polymer science, photochemistry, theoretical physics and chemistry, so on. The research center will continue to make efforts to push forward international and domestic collaborative research.

April, 2018

Keisuke Tominaga
Director of Molecular Photoscience Research Center,
Kobe University

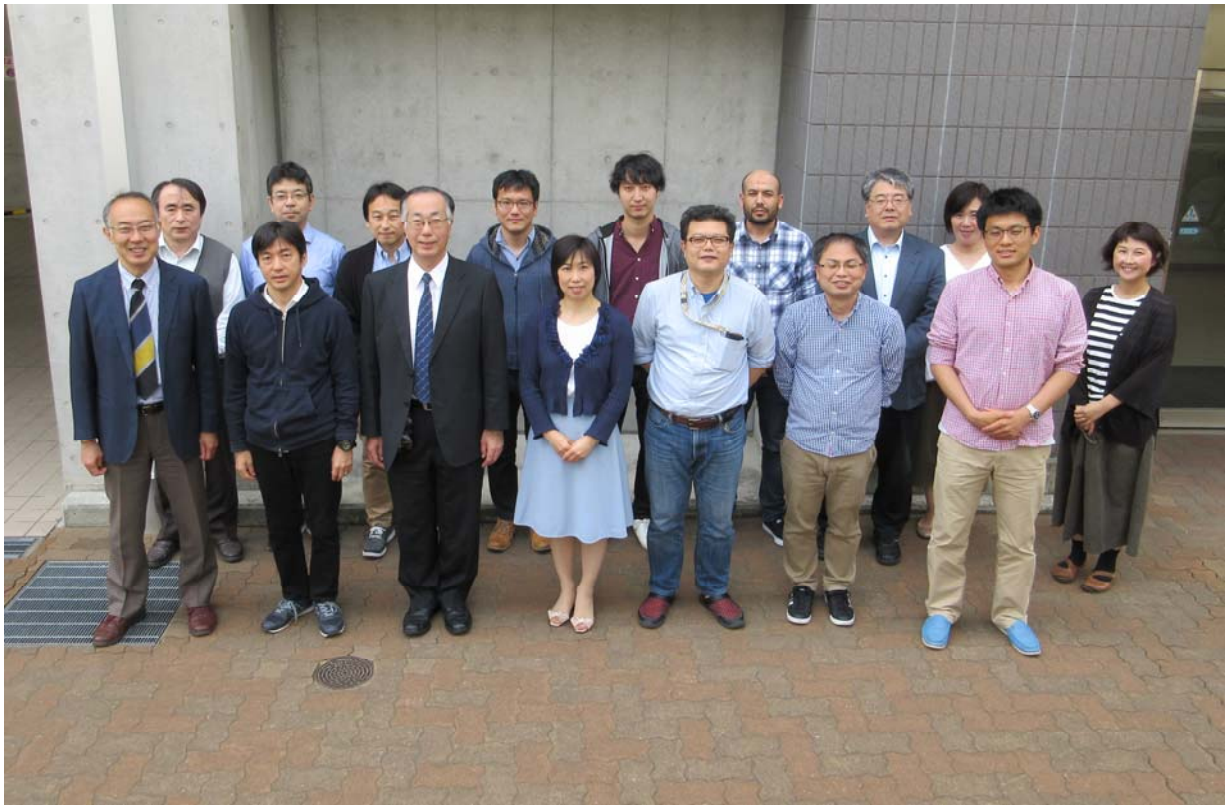

Contents

Members	5
Research Activities	
Laser Molecular Photoscience Laboratory	6
Terahertz Molecular Chemistry Laboratory	21
Terahertz Material Physics Laboratory	37
Original Papers	52
Invited Talks	56
Presentation at Conferences (International and domestic)	59
Presentation by Graduate Students and Postdocs	62
Books	69
Other Publications	70
Lectures to Public	71
Awards	72
Conference Organization	73
Seminars	74

Members

Keisuke Tominaga	Director
Hitoshi Ohta	Vice-Director

Takako Miyazaki	Assistant
Sachiyo Tombe	Assistant
Kei Kita	Assistant

Laser Molecular Photoscience Laboratory

Yasuhiro Kobori	Professor
Shunji Kasahara	Associate Professor
Takashi Tachikawa	Associate Professor
Hiroki Nagashima	JSPS Postdoctoral Fellow
Daphné Lubert-Perquel	Kobe University Visiting Research Fellow (October ~ November 2017)

Terahertz Molecular Chemistry Laboratory

Keisuke Tominaga	Professor
Kaoru Ohta	Research Associate Professor
Feng Zhang	Postdoctoral Fellow
Masaki Okuda	JSPS Postdoctoral Fellow
Alvin Karlo Garcia Tapia	Kobe University Visiting Research Fellow (January ~ March 2018)
Lou Serafin Lozada	Kobe University Visiting Research Fellow (March 2018)
Harumi Sato	Associate Professor (Supplementary assignment. Main assignment is Graduate School of Human Development and Environment)

Coherent Photoscience Laboratory

Hitoshi Ohta	Professor
Susumu Okubo	Associate Professor
Khalif Benzid	Postdoctoral Fellow
Keigo Hijii	Researcher
Toshiro Kohmoto	Professor (Supplementary assignment. Main assignment is Graduate School of Science)
Eiji Ohmichi	Associate Professor (Supplementary assignment. Main assignment is Graduate School of Science)

I. Laser Molecular Photoscience Laboratory

I-A. SPIN INTERACTIONS STUDIED BY TIME RESOLVED MAGNETIC RESONANCE SPECTROSCOPY

In the natural photosynthesis, the organic solar cells and the photocatalysis, transient radical species or carriers are immediately generated by the light-induced chemical reactions for the photo-energy conversion, providing essential sources of the living energies. However, it has been unclear how those transient molecules are initially interacting each other before the carrier-conductions or charge-dissociation take place. In our group, we are developing experimental methodologies to determine molecular positions, orbital orientations and orbital overlap (electronic coupling) in the initially generated radical-pairs, multiexcitons, and electron-hole pairs in the photoactive proteins, in the solar cells, and in the photocatalysis on the basis of the transient electron paramagnetic resonance (EPR) method. We have clarified several fundamental mechanisms of the energy-conversions in the singlet-fission materials and in the low band gap polymer systems.

Formation of Distinct Quintet States in Ordered Organic Semiconductor Films

Daphné V. Lubert-Perquel[1], Enrico Salvadori[2], Matthew Dyson[1], Paul N. Stavrinou[3], Riccardo Montis[1], Hiroki Nagashima, Yasuhiro Kobori, Sandrine Heutz[1] and Christopher W. M. Kay[2]

[1]Imperial College London, [2]University College London, [3]Oxford University,

(arXiv:1801.00603 2017)

The growing interest in harnessing singlet fission for photovoltaic applications stems from the possibility of generating two excitons from a single photon. Quantum efficiencies above unity have been reported, yet the correlation between singlet fission and intermolecular geometry is poorly understood. To address this, we investigated ordered solid solutions of pentacene in p-terphenyl grown by organic molecular beam deposition. Two classes of dimers are expected from the crystal structure – parallel and herringbone – with intrinsically distinctive electronic coupling. Using Electron Paramagnetic Resonance (EPR) spectroscopy, we provide compelling evidence for the formation of distinct quintet excitons at room temperature. These are assigned to specific pentacene pairs according to their angular dependence. This work highlights the importance controlling the intermolecular geometry and the need to develop adequate theoretical models to account for the relationship between structure and electronic coupling in strongly coupled high-spin states.

The orientation of the pentacene molecules was investigated as a function of concentration and the results for the molecular *x*-axis parallel to the magnetic field are shown in Figure 1a. Figure 1b, reports a 2D mapping of the TREPR spectrum of the 10% pentacene: p-terphenyl blended film. Four pairs of peaks are visible, with the two inner peak separations about 1/3 of the outer peak separations. This suggests two pairs of strongly exchanged coupled triplets ($J > D$), forming

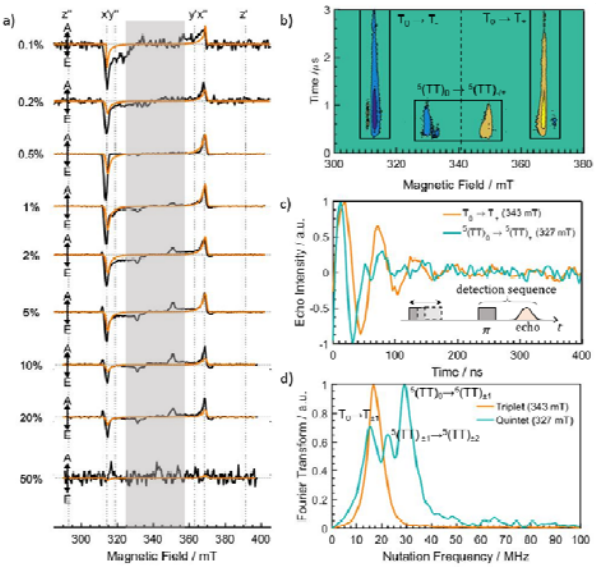

Figure 1. Identifying quintet states at room temperature via EPR spectroscopy and nutation experiments of the (TT) and isolated T states. a) The x-orientation as a function of pentacene concentration with the simulated data shown in orange. The inner peaks are believed to belong assigned to long-lived strongly coupled triplet states. b) Tr-EPR of the 10% pentacene in p-terphenyl 1um film. The (TT) states (inner peaks), appear earlier in time than the isolated T states (outer peaks), formed by dissociation or ISC. c) Nutation experiment for the high-field quintet and triplet transitions, with the pulse sequence shown in the inset. d) Fourier Transform of the data showing a ratio of 1.74 in accord with the nominal value of $\sqrt{3} = 1.73$.

quintet states with $S = 2$. The quintet lifetime of the innermost peaks (334 and 349 mT indicated by short blue arrows in Figure 1b), which is most apparent in the emissive line, is ~300 ns, and its decay coincides with a rise in the corresponding outer strong triplet signals (315 and 369 mT indicated by black arrows in Figure 1b). This suggests a short-lived high-spin state that efficiently separates into free triplets, which in turn is very long-lived (> 3 µs). On the other hand, the second pair of quintets (331 and 351 mT) has lifetime of ~1 µs and appears to coexist with the weak, outermost triplet signals (312 and 372 mT). This could result from a thermally activated equilibrium between the quintet and triplet states.

The most conclusive way to determine the spin state of the species giving rise to the peaks observed in the TR-EPR surface is to perform transient nutation measurements at the relevant field positions. The observed frequencies directly depend on the total spin (S) and on the m_S component and therefore allow for a definitive assignment of the different transitions. The explicit formula correlating the nutation frequency (ω) to the total spin (S) and the spin projections characteristic of the transition observed (m_S and $m_{S\pm1}$) reads:

$$\omega = \omega_{1/2} \sqrt{\{S(S+1) - m_S (m_{S\pm1})\}} \quad (1)$$

where $\omega_{1/2} = g\mu_B B_1/\hbar$ is the precession frequency for a spin S = 1/2 and B_1 is the microwave field strength. It follows that for transitions from the $m_s = 0$ state, the ratio of Rabi frequencies for pure quintet and triplet states is $\sqrt{3}$. Conversely, for transitions from the $m_S = 1$ the ratio equates to $\sqrt{2}$. Comparison between measurements at different field positions but with all the other experimental settings unchanged (note that nutation frequencies depend on the strength of B_1 and therefore on the Q factor) provides a way of probing the spin state of the observed transitions. Figure 1c,d shows the nutation frequency and corresponding Fourier transform of the long-lived triplet and quintets at the high-field position. The FFT shows the triplet and corresponding quintet nutation frequency with a ratio of $\sqrt{3}$, as well as an intermediate

peak with ratio $\sqrt{2}$. This former contribution is an S_0 to $S\pm1$ transition and the latter is a $S\pm1$ to $S\pm2$ transition. This indicates the high spin states of the quintet are also populated in this system.

At increasing concentrations pairs of pentacene molecules are more likely to form increasing the probability of singlet fission occurring. Moreover, dilution inhibits excitation/spin diffusion significantly enhancing the excitation lifetime. We have provided the first direct evidence of two distinct electronic coupling schemes that can be assigned to pairs of pentacenes on the basis of their relative orientations. This unambiguously proves that the structure of the pentacene dimers directly affects the properties and dynamics of the corresponding triplet and quintet high-spin states and that specific geometries are likely to promote the efficiency of SF and to extend the lifetime of the triplet excitons.

Time-Resolved EPR Study on Photoinduced Charge-Transfer Trap State in Thiophene-Thiazolothiazole Copolymer Film

Yuta Yamamoto, Takumi Ako, Takashi Tachikawa, Itaru Osaka[1] and Yasuhiro Kobori

[1]Hiroshima University

(*J. Photopolymer. Sci. Tech.* 2017)

To shed a light on fundamental optoelectronic properties of conjugated polymer films applicable to the organic photovoltaics (OPV), field-effect transistors (FET) and light-emitting diodes (LED), we have characterized interspin separation and exchange coupling of interchain charge-transfer (CT) states in a pristine film of thiophene–thiazolothiazole copolymer (PTzBT–BOHD) by using the time-resolved EPR method. It has been indicated that the CT state is generated at the disordered regions of the polymer films as deep trap sites via the singlet−exciton diffusion in polymer amorphous phase. These characteristics of the trapped charges may limit the device performances in the OPV, FET and LED applications and thus are informative for the device developments.

Figure 1a shows TREPR spectra of the pristine films of PTzBT–BOHD measured at 77 K. The negative signal denoted by 'E' is the TREPR intensity (transverse magnetization) by the microwave emission. The spectrum shapes are composed of a sharp peak around 337 mT and a broad signal ranging from 335.5 to 338 mT. In the previous TREPR study, the transient radical pairs were reported to be generated as microwave emissions in regioregular poly(3-hexylthiophene) –fullerene (P3HT–C_{60}) linked dyad molecules. The net E polarization was well explained by the photoinduced charge-separation (CS) via the triplet exciton in the P3HT moiety. Thus, the present emissive signals around $g = 2$ indicate that the CT state is produced in the pristine film as the triplet

Figure 1b shows time profile of the transient EPR intensity at 337.2 mT. The E polarization persists more than 5 μs which is attributable to the spin-lattice relaxation time (T_1). This is ten times larger than the reported T_1 = 0.5 μs in the photoinduced CS state generated at the BHJ domain interfaces in the RR–P3HT:PCBM blends at T = 77 K. This denotes that the charge motions are highly restricted in the present film,

suggesting that the charges in the CT state exist as deep trap sites rather than mobile charges to contribute to the photocurrent generation.

To characterize the geometry and the electronic interaction of the CT state, we computed the delay time dependence of the transient EPR signals as shown by the gray lines in Figure 1a based upon the spin correlated radical pair (SCRP) model utilizing the above g-factors and the hyperfine coupling constants with considering the spin density distribution.

The spectrum shapes were well reproduced by setting the dipolar coupling parameter of D = –0.8 mT and J = –0.5 mT, as shown by the grey lines in Figure 1a. From D = –0.8 mT, the center-to-center separation (r_{CC}) between the charges is estimated to be 1.5 nm in the present CT state. In the previous study, the photoinduced CS states generated at the BHJ domain interfaces were characterized to be J = +6 μT for r_{CC} = 1.5 nm in the RR–P3HT:PCBM blends at T = 77 K. This significantly weak J coupling was explained by a weakened electronic coupling (V) between the charges due to highly delocalized distributions in the unpaired orbitals of the mobile holes at the polymer crystalline phase. On the other hand, the present strong J coupling denotes that the photoinduced charges in the CT state is rather localized to strengthen the orbital overlap. However, a highly strong coupling of J > 3 mT was obtained for a larger r_{CC} of 1.8 nm in the covalently linked dyad of $P3HT^{+\bullet}$–$C_{60}^{-\bullet}$. Thus, the present J coupling is not in line with an intrachain CT ($P^{+\bullet}$–$P^{-\bullet}$) generation within the polymer backbone but the interchain CT state ($P^{+\bullet}$ $P^{-\bullet}$). The stronger J of –0.5 mT than in the RR–P3HT:PCBM interface is well consistent with

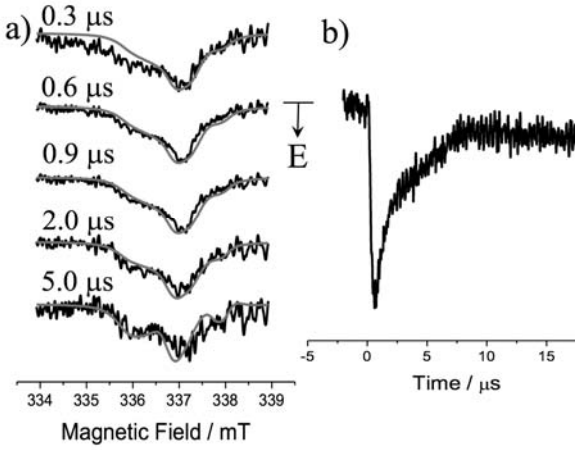

Figure 1. (a) Delay time dependence of the TREPR spectrum of the as-spun pristine film of PTzBT–BOHD obtained by the 532 nm laser excitation at T = 77 K. (b) Time profile of the EPR intensity at 337.2 mT. precursor CS. We performed the molecular orbital calculations of the monomer unit of PTzBT–BOHD for the radical cation ($P^{+\bullet}$) and the radical anion ($P^{-\bullet}$) at the B3LYP/6-31G (d,p) level with the NMR GIAO method to obtain the g–tensors and the hyperfine tensors. (g_X, g_Y, g_Z) = (2.0018, 2.0026, 2.0021) for $P^{+\bullet}$ and (g_X, g_Y, g_Z) = (2.0085, 2.0050, 2.0019) for $P^{-\bullet}$ were obtained as principal values. The small g-anisotropy in $P^{+\bullet}$ and the larger g-anisotropy in $P^{-\bullet}$ are both coincident with the coexistence of the sharp (at 337.2 mT) and broad spectrum components in Figure 2a, strongly supporting the above hypothesis of the CT generation. It is noted that the spectrum width obtained by the above anisotropies in the g-factors and the hyperfine couplings were smaller for the isolated radicals than the field range from 335.5 to 338 mT in Figure 1a, indicating that the spin-spin dipolar interaction (d) and the exchange coupling (J) between the charges also contribute to the entire spectrum shapes. No other TREPR bands were obtained at a wider field-scan experiment for the pristine film.

the above argument that the interchain CT states are not located at the dominant polymer crystalline phase but at minor disordered regions, as shown at the upper left in Figure 2, generating the long–lived deep trap site in the pristine polymer film.

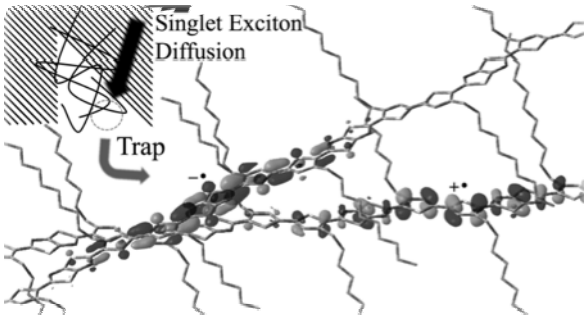

Figure 2. Image view of the geometry of the photoinduced CT state as the localized charges separated by 1.5 nm that explain the TREPR spectra and the large spin-lattice relaxation time in Figure 2 at T = 77 K. The exciton-diffusion represented by a dark black arrow may result in the trapped-CT state following the ISC at the disordered region, as shown at the upper left.

Time-Resolved EPR Study on Charge Dynamics of Electron-Hole Pairs in Lead Iodide Perovskite Thin Film

Yasuhiro Kobori

(*2017 231st ECS meeting USA, Invited*)

For developments of the light-energy conversion systems, it is essential to achieve efficient long-range charge-separations (CS). Light-induced electrons and holes generated by the electron-transfer (ET) reactions are thus required to escape from the electrostatic binding at the initial stage. In this respect, the lead iodide perovskite solar cells have attracted great attentions since they exhibit quite efficient energy conversion performances. This solar cell adopts the hybrid metal iodide perovskites as a photoactive layer with the general formulation of ABX_3($CH_3NH_3PbI_3$), where A is the methyl-ammonium ($CH_3NH_3^+$) cation, B is Pb^{2+} and M is I^-. In the devise structure, this photoactive layer is sandwiched by the compact titanium oxide (TiO_2) layer and by the hole-transporting layer to efficiently collect the photocarriers generated by the light irradiations of the perovskite, giving rise to ~20% power conversion efficiencies (PCE).

Recent studies have clearly shown that the carrier mobilities of the electrons and the holes are significantly high in the $CH_3NH_3PbI_3$ layer, resulting in micrometer ranges of the charge-diffusion lengths. [1] These efficient charge diffusions play a crucial role on the prevention of the unwanted geminate charge-recombination in the electron-hole pairs. However, little is known concerning the electronic interactions of the electron-hole pairs initially generated in the $CH_3NH_3PbI_3$ layer. At lower temperature (T < 160 K), it is reported that the electron and the hole generated by the light irradiation exhibit a Wannier exciton character with a biding energy of ~30 meV. [2] Thus, low temperature investigations of the electronic characters in the electron-hole pairs are very

important to understand the mechanisms of the efficient charge-conductions initiated by the primary electron-hole pairs in the $CH_3NH_3PbI_3$ layer. Another importance is to understand electronic characters of the trapped-charges generated by the light irradiations of the photoactive layers. It is recently reported that the charge careers are trapped at the surface area of the crystalline $CH_3NH_3PbI_3$ layer. [3] However, electronic orbital characteristics of the trapped charges are not well known in the devices.

Time-resolved electron paramagnetic resonance (TREPR) and pulsed EPR methods have been powerful to obtain the electron spin-spin interactions including the spin-spin exchange coupling of the photoinduced CS states and thus have been utilized to characterize the interspin distances and the electronic couplings of the transient CS states. [4] Additionally, TREPR can detect the electron spin polarization (ESP) as an effect of the initial photochemical events. This phenomenon is referred to as the chemically induced dynamic electron polarization (CIDEP). According to the radical pair mechanism (RPM) CIDEP, the ESP is generated as a result of the coherent singlet-triplet interconversion in the presence of the exchange coupling (*J*) of the primary radical-pair states, producing the enhanced microwave absorption and the microwave emission in the separated radicals during the diffusive separations of the individual radicals in the radical-pair.[5] Since the ESP detected as the microwave absorption (A) or the emission (E) is thus sensitive to *J*, one is able to access the electronic interactions in the primary radical-pairs.[6]

To unveil the above fundamental electronic characteristics for the light-induced charge conductions, we have observed low temperature TREPR spectra for the three layer thin films (Spiro-OMeTAD/$CH_3NH_3PbI_3$/TiO_2 on a glass substrate) composed of the organic hole transport layer (Spiro-OMeTAD), the $CH_3NH_3PbI_3$ layer and the mesoporous TiO_2 fabricated by spin coating method on the mesoporous TiO_2 films. From the EPR spectra, we have characterized the spin density distributions of the trapped holes of the $CH_3NH_3PbI_3$ layer at 110 K from the anisotropic hyperfine structures originating from the iodine atoms (I). Furthermore, from the ESP generated in the trapped hole, we estimated the J coupling in the primary electron-hole pairs which will give us an insight on the electronic coupling of the Wannier excitons.

[1] . Xing, G.; Mathews, N.; Sun, S.; Lim, S. S.; Lam, Y. M.; Grätzel, M.; Mhaisalkar, S.; Sum, T. C. *Science* **2013**, *342*, 344.

[2] . Yamada, Y.; Nakamura, T.; Endo, M.; Wakamiya, A.; Kanemitsu, Y. *J. Am. Chem. Soc.* **2014**, *136*, 11610-11613.

[3] . Tachikawa, T.; Karimata, I.; Kobori, Y. *J. Phys. Chem. Lett.* **2015**, *6*, 3195-3201.

[4] Kobori, Y.; Miura, T. *J. Phys. Chem. Lett.* **2015**, *6*, 113-123.

[5] . Kobori, Y.; Yago, T.; Akiyama, K.; Tero-Kubota, S.; Sato, H.; Hirata, F.; Norris, J. R. *J. Phys. Chem. B* **2004**, *108*, 10226-10240.

[6] Kobori, Y.; Yamauchi, S.; Akiyama, K.; Tero-Kubota, S.; Imahori, H.; Fukuzumi, S.; Norris, J. R. *Proc. Natl. Acad. Sci. U. S. A.* **2005**, *102*, 10017-10022.

Electron spin polarization imaging applied to primary charge separation in the PSII

Yasuhiro Kobori

(*2017 The 5th Awaji International Workshop on Electron Spin Science & Technology* (*AWEST2017*)*, Invited*)

In the primary event of the photosynthesis by green plants and cyanobacteria, the light energy is transferred through antenna complexes to the reaction center (RC) of the photosystem II (PSII) in the thylakoid membrane. The RC is composed of the D1/D2 heterodimer, possessing the chlorophyll a (Chla) pair (P_{D1}/P_{D2}), the accessory Chla (Chl_{D1}/Chl_{D2}), the pheophytins ($Pheo_{D1}/Pheo_{D2}$), two quinones, and two additional Chla molecules as the redox active cofactors. It has been suggested that the electron is transferred to $Pheo_{D1}$ from $^1Chl_{D1}$* electronically excited via the antenna, following hole-transfer to the "special pair (P)" of P_{D1}/P_{D2} generating the primary charge-separated (CS) state of $P^{+\bullet}$ $Pheo_{D1}^{-\bullet}$. Several studies have been performed to understand mechanisms of an extremely high redox potential of $P^{+\bullet}$ in PSII while the photosynthetic reaction centers (PRC) do not have such potentials in purple bacteria. For chemically oxidized PSII RC samples, the cationic charge is known to be localized on the D1 part (P_{D1}) at 70-80 % over P_{D1}/P_{D2}, lowering the singly occupied molecular orbital (SOMO) level to oxidize the Mn_4CaO_5 cluster. On the primary CS state, Matysik et al. [1] demonstrated that the cationic charge is localized at a single Chla site by using the photo-CIDNP method.

In the primary CS states, the above oxidative and localized cationic charge would cause a strong electronic interaction in $P_{D1}^{+\bullet}$ $Pheo_{D1}^{-\bullet}$ and thus suffer from an energy-wasting CR process, since the distance (1.5 nm) between $P_{D1}^{+\bullet}$ and $Pheo_{D1}^{-\bullet}$ is expected to be shorter than the CS distance of 1.8 nm in *Rhodobacter sphaeroides* [2] in which the hole distribution is highly delocalized on the special pair. However, a lifetime of 200 ns was obtained for the primary CS state in the quinone doubly-reduced membrane of PSII, while lifetime = 25 ns is significantly shorter in *Rhodobacter sphaeroides*. On this, no experimental studies have been performed to understand how cofactor geometries play roles on the electronic interaction of the primary CS state in which the anionic charge may significantly influence the electronic state.

We have observed the primary CS states in quinone pre-reduced membranes of PSII from spinach in frozen solution and in oriented multilayers at 77 K using an X-band time-resolved EPR (TREPR) method. Herein, we propose a novel method of "3D spin polarization imaging" by which the anisotropic spin polarization is mapped to all possible magnetic field directions from the powder-pattern TREPR to obtain geometries of the primary CS state [3]. We also show that the electronic coupling between the charges is significantly weak although the tunneling route is geometrically active after the primary charge-separations [3].

[1] J. Matysik et al. *Proc. Natl. Acad. Sci. U. S. A.* **2000,** *97,* 9865-9870.

[2] Y. Kobori, J. R. Norris, et al. *J. Phys. Chem. C* **2015,** *119,* 8078-8088.

[3] M. Hasegawa, H. Nagashima, R. Minobe, T. Tachikawa, H. Mino, Y. Kobori *J. Phys. Chem. Lett.* **2017**, *8* 1179-1184.

Electron Spin Polarization Imaging of Photoinduced Primary Charge-Separated States in PSII

Yasuhiro Kobori

(*2017 Spin Chemistry Meeting, Invited*)

In the primary event of the photosynthesis by green plants and cyanobacteria, the light energy is transferred through antenna complexes to the reaction center (RC) of the photosystem II (PSII) in the thylakoid membrane. The RC is composed of the D1/D2 heterodimer, possessing the chlorophyll a (Chla) pair (P_{D1}/P_{D2}), the accessory Chla (Chl_{D1}/Chl_{D2}), the pheophytins ($Pheo_{D1}/Pheo_{D2}$), two quinones, and two additional Chla molecules as the redox active cofactors. It has been suggested that the electron is transferred to $Pheo_{D1}$ from $^1Chl_{D1}$* electronically excited via the antenna, following hole-transfer to the "special pair (P)" of P_{D1}/P_{D2} generating the primary charge-separated (CS) state of $P^{+\bullet}$ $Pheo_{D1}^{-\bullet}$. Several studies have been performed to understand mechanisms of an extremely high redox potential of $P^{+\bullet}$ in PSII while the photosynthetic reaction centers (PRC) do not have such potentials in purple bacteria. For chemically oxidized PSII RC samples, the cationic charge is known to be localized on the D1 part (P_{D1}) at 70-80 % over P_{D1}/P_{D2}, lowering the singly occupied molecular orbital (SOMO) level to oxidize the Mn_4CaO_5 cluster. On the primary CS state, Matysik et al. [1] demonstrated that the cationic charge is localized at a single Chla site by using the photo-CIDNP method.

In the primary CS states, the above oxidative and localized cationic charge would cause a strong electronic interaction in $P_{D1}^{+\bullet}$ $Pheo_{D1}^{-\bullet}$ and thus suffer from an energy-wasting CR process, since the distance (1.5 nm) between $P_{D1}^{+\bullet}$ and $Pheo_{D1}^{-\bullet}$ is expected to be shorter than the CS distance of 1.8 nm in *Rhodobacter sphaeroides* [2] in which the hole distribution is highly delocalized on the special pair. However, a lifetime (τ) of 200 ns was obtained for the primary CS state in the quinone doubly-reduced membrane of PSII, while τ = 25 ns is significantly shorter in *Rhodobacter sphaeroides*. On this, no experimental studies have been performed to understand how cofactor geometries play roles on the electronic interaction of the primary CS state in which the anionic charge may significantly influence the electronic state.

We have observed the primary CS states in quinone pre-reduced membranes of PSII from spinach in frozen solution and in oriented multilayers at 77 K using an X-band time-resolved EPR (TREPR) method. Herein, we propose a novel method of "3D spin polarization imaging" by which the anisotropic spin polarization is mapped to all possible magnetic field directions from the powder-pattern TREPR to obtain geometries of the primary CS state.[3] We also show that the electronic coupling between the charges is significantly weak although the tunneling route is geometrically active after the primary charge-separations [3].

[1] J. Matysik et al. *Proc. Natl. Acad. Sci. U. S. A.* **2000,** *97,* 9865-9870.

[2] Y. Kobori, J. R. Norris, et al. *J. Phys. Chem. C* **2015,** *119,* 8078-8088.

[3] M. Hasegawa, H. Nagashima, R. Minobe, T. Tachikawa, H. Mino, Y. Kobori *J. Phys. Chem. Lett.* **2017** *8,* 1179-1184.

Time-Resolved EPR Study on Photoinduced Charge-Transfer Trap States in Thiophene-Thiazolothiazole Copolymer Films

Yasuhiro Kobori, Yuta Yamamoto, Takumi Ako, Takashi Tachikawa, Itaru Osaka[1]

[1]Hiroshima University

(*2017 11th Japanese-Russian Workshop on Open Shell Compounds and Molecular Spin Devices*, *Invited*)

Great attentions have been attracted on the organic photovoltaic (OPV) devices as the next generation thin-film solar cells that can be low-cost, flexible and light. [1] Conjugated polymers have extensively been utilized in various organic electronic devices including the solar cells, field-effect transistors (FET) [2] and light-emitting diodes [3] (LED). The spin coating method from mixed solutions consisting of the conjugated polymers as the electron donors (D) and fullerene derivatives as the acceptors (A) has been employed to produce the solid photoactive layer of the OPV cells [1]. In the organic photoactive layers, it is well known that the polymer molecules are self-organized to generate the bulk heterojunction (BHJ) [4] interfaces. Apart from the OPV applications, pristine films of the conjugated polymers are also utilized for the FET and LED applications [5]. The polymers usually form two dimensional lamellae structures as a result of close interchain packing interaction.[4] Such crystalline phases are known to play a key role for the mobilities of the charges and the excitons in the organic devices. Recent studies suggested that non-fluorescent CT characters exist as a competitive channel of the formation of emissive exciton-type states and determine the light emission efficiencies of the LED films [5].

Despite the significance of the non-fluorescent CT state, no study has experimentally characterized geometry and electronic character of the photoinduced CT state in the pristine polymer films. Consequently, the optoelectric properties of the polymer films have not been fully understood. In this study, we have directly observed the photoinduced CT state for a pristine film by thiophene–thiazolothiazole copolymer (PTzBT–BOHD in Fig.1) [6] fabricated by the spin–coating method using time-resolved EPR (TREPR) method to characterize the orbital geometries, the electronic property of the polymer CT state. We show that a long-lived interchain CT states ($P^{+\bullet}$ $P^{-\bullet}$) are generated as a trap state at disordered region as defects at a cryogenic temperature.

[1] G. Yu, J. Gao, J. C. Hummelen, F. Wudl and A. J. Heeger, *Science* **270** (1995) 1789.

[2] C. B. Nielsen and I. McCulloch, *Prog. Polym. Sci.* **38** (2013) 2053.

[3] I. F. Perepichka, D. F. Perepichka, H. Meng and F. Wudl, *Adv. Mater.* **17** (2005) 2281.

[4] Y. Kim, S. Cook, S. M. Tuladhar, S. A. Choulis, J. Nelson, J. R. Durrant, D. D. C. Bradley, M. Giles, I. Mcculloch, C. S. Ha and M. Ree, *Nat. Mater.* **5** (2006) 197.

[5] Z. J. Hu, A. P. Willard, R. J. Ono, C. W. Bielawski, P. J. Rossky and D. A. Vanden Bout, *Nat. Commun.* **6** (2015) 8246.

[6] I. Osaka, M. Saito, T. Koganezawa and K. Takimiya, *Adv. Mater.* **26** (2014) 331.

I-B. SINGLE-MOLECULE STUDIES ON PHOTO-ENERGY CONVERSION PROCESSES

To design a more efficient solar energy conversion system (light energy to electrical or chemical energy), it is important to reveal and understand the mechanisms of various chemical reactions at heterogeneous interfaces. We have investigated the photochemical and photophysical processes occurring on a variety of light energy conversion systems such as photocatalysis and solar cells using advanced single-molecule, single-particle spectroscopy techniques and gain new insights related to spatial and temporal heterogeneities in reactions and structures, which are always masked by ensemble averaging.

Direct Observation of Charge Collection at Nanometer-Scale Iodide-Rich Perovskites during Halide Exchange Reaction on $CH_3NH_3PbBr_3$

Izuru Karimata, Takashi Tachikawa, and Yasuhiro Kobori

(*J. Phys. Chem. Lett., 2017*)

Organolead halide perovskites $MAPbX_3$ (MA = $CH_3NH_3^+$, X = Cl^-, Br^-, or I^-) have emerged as a promising class of materials for solar cell applications as well as optoelectronic devices and are known to undergo reversible halide exchange reactions, enabling bandgap tuning over the visible light region. Using single-particle photoluminescence (PL) imaging for in situ observation, we have studied the structure-dependent charge dynamics during halide exchange with iodide ions on an $MAPbBr_3$ crystal. In particular, as shown in Figure 1, we optically detected nanometer-scale iodide-rich domains (i.e., $MAPbBrI_2$). To characterize the kinetics of individual domains, a statistical analysis of the characteristic time (τ_{on}) during which persistent emission is exhibited was examined. From the analysis, we found that their lifetimes of several tens of milliseconds are limited by reaction with diffusing vacancies. Furthermore, it was discovered that the bursts were occasionally accompanied by strong emission with a narrow line width and a slightly red-shifted peak below the main peak. The domains effectively collect the charge carriers from the bulk crystal, thus resulting in amplified spontaneous emission (ASE) under continuous-wave laser irradiation. These results suggest that efficient charge extraction in the perovskite solar cell is achievable by introduction of iodide-rich domains near the surface of $MAPbBr_3$ film. Our findings will provide direction for development of perovskite heterostructures with enhanced charge utilization.

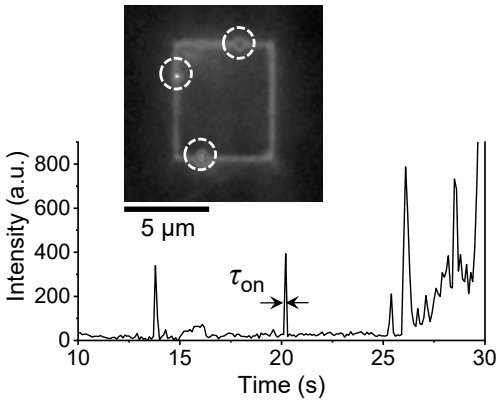

Figure 1. A typical PL intensity trajectory showing the bursts. Inset indicates burst emission spots (marked by red circles) on a single $MAPbBr_3$ crystal during the halide exchange reaction.

Topotactic Epitaxy of $SrTiO_3$ Mesocrystal Superstructures with Anisotropic Construction for Efficient Overall Water Splitting

Peng Zhang,[1] Tomoya Ochi, Mamoru Fujitsuka,[1] Yasuhiro Kobori, Tetsuro Majima[1], Takashi Tachikawa

(*Angew. Chem. Int. Ed., 2017*)

[1]Osaka University

Mesocrystals are superstructures with a crystallographically ordered alignment of nanoparticles. Owing to their organized structures, mesocrystals have unique characteristics such as a high surface area, pore accessibility, and good electronic conductivity. A novel perovskite $SrTiO_3$ mesocrystal superstructure with well-defined orientation of assembled cubic nanocrystals was synthesized by topotactic epitaxy from TiO_2 mesocrystals through a facile hydrothermal treatment. The $SrTiO_3$ mesocrystal exhibits three times the efficiency for the hydrogen evolution of conventional disordered systems in alkaline aqueous solution. It also exhibits a high quantum yield of 6.7% at 360 nm in overall water splitting and even good durability up to 1 day. Temporal and spatial spectroscopic observations revealed that the synergy of the efficient electron flow along the internal nanocube network and efficient collection at the larger external cubes produces remarkably long-lived charges for enhanced photocatalysis. The design principle of perovskite-type mesocrystals and the mechanistic insight into the heterogeneous charge transfer reactions occurring in the superstructure system will provide new strategies for the fields of photocatalysis and optoelectronics.

The Development of Functional Mesocrystals for Energy Harvesting, Storage, and Conversion

Peng Zhang,[1] Takashi Tachikawa, Mamoru Fujitsuka,[1] Tetsuro Majima[1]

(*Chem. -Eur. J., 2018*)

[1]Osaka University

Higher-ordered semiconductors have attracted extensive research interest as an adopted engineering for active solar energy harvesting, storage, and conversion. It is well-known that the effective separation and anisotropic migration of photogenerated charges are the basic driven force required for superior efficiency. However, the morphology and stoichiometric variation of these semiconductors play essential roles in their physicochemical properties of bulk and surface, especially for efficient interparticle or interfacial charge transfer. To this point, the strategy of controlling the topotactic transformation toward superstructures with optimized functionality is preferable for a wide range of optoelectronic and catalytic engineering applications. In this Minireview, we provide an overview of the crystal orientation, synthetic engineering, functional applications, and spatial and temporal charge dynamics in TiO_2 mesocrystals and others. The viewpoint of in-depth understanding of the structure-related kinetics would offer an opportunity for design of versatile mesocrystal semiconductors sought-after for potential applications.

I-C. HIGH-RESOLUTION SPECTOSCOPY OF POLIATOMIC MOLECULES

Doppler-free high-resolution spectroscopic techniques are powerful tools for studying the structure and dynamics of excited polyatomic molecules in detail and unambiguously. Single-mode auto-scan laser systems in UV-Visible region, the absolute wavenumber measurement system, and several Doppler-free high-resolution spectroscopic measurement systems have been constructed to investigate the excited molecules. High-resolution and high-accuracy measurement of the spectral lines enable to observe rotationally-resolved electronic transition and to find out the excited state dynamics such as internal conversion (IC), intersystem crossing (ISC), and intramolecular vibrational redistribution (IVR) through the fairly deviation of the spectral line position, intensity anomaly and the change of the spectral linewidth. Recently, we observed the high-resolution spectrum and Zeeman effects of the π-π* transition of several aromatic molecules such as benzene, naphthalene, anthracene, etc. and these molecular constants were determined in high-accuracy. We have observed the high-resolution spectrum of 2-Cl naphthalene and 1-Cl naphthalene, which are expected to find the spin-orbit interaction (ISC) from the heavy-atom effect. We also observed the high-resolution spectrum of fluorene $S_1 \leftarrow S_0$ transition, and determined these molecular constants and found the local perturbation in the vibrational excited state of S_1.

Rotationally-resolved High-resolution Laser Spectroscopy of Fluorene

Shinji Kuroda and Shunji Kasahara

(*International Symposium on "Diversity of Reaction Dynamics, 2017*)

High-resolution laser spectroscopy is very powerful to study the molecular structure and excited state dynamics in detail and unambiguously. We established the single-mode UV laser system, and measured the high-resolution spectra of several polyatomic molecules in UV region. As for fluorene, high-resolution spectra of the lowest three vibronic bands of the $S_1 \leftarrow S_0$ transition have already been reported by J. T. Yi [1], but the excited state dynamics has not been discussed. In purpose of understanding the exited state dynamics of fluorene, we have observed rotationally-resolved high resolution spectra of the $S_1{}^1B_2 \leftarrow S_0{}^1A_1$ transition, and the Zeeman effect has been observed.

A molecular beam was obtained by expanding of fluorene vapor with Ar gas through a pulsed nozzle into the vacuum chamber and collimated by using a skimmer and a slit. High-resolution fluorescence excitation spectra were measured by crossing a single-mode UV laser beam perpendicular to a collimated molecular beam.

High-resolution fluorescence excitation spectra of seven vibronic bands have been observed. In the observed region, the typical linewidth is about 25 MHz. From the pattern of the spectra, we found that all bands are the *a*-type transition (selection rule: $\Delta K=0$, $\Delta J=0$, ± 1), whose transition moment is parallel to the long axis of the molecule. In each bands, rotational lines were assigned, and their molecular constants were determined with high accuracy. We show high-resolution spectrum

of the 0_0^0 + 204 cm^{-1} band in Figure 1. In this band, we succeeded to find systematic deviation between the observed and calculated spectrum in some rotational lines, which is attributed to perturbation with another vibronic level in S_1 state. We have measured the high-resolution spectrum under the external magnet field up to 1.2 T. However, the Zeeman effect was not found.

[1] J. T. Yi, L. Alvarez-Valtierra, D. W. Pratt, *J. Chem. Phys.* **124**, 244302 (2006).

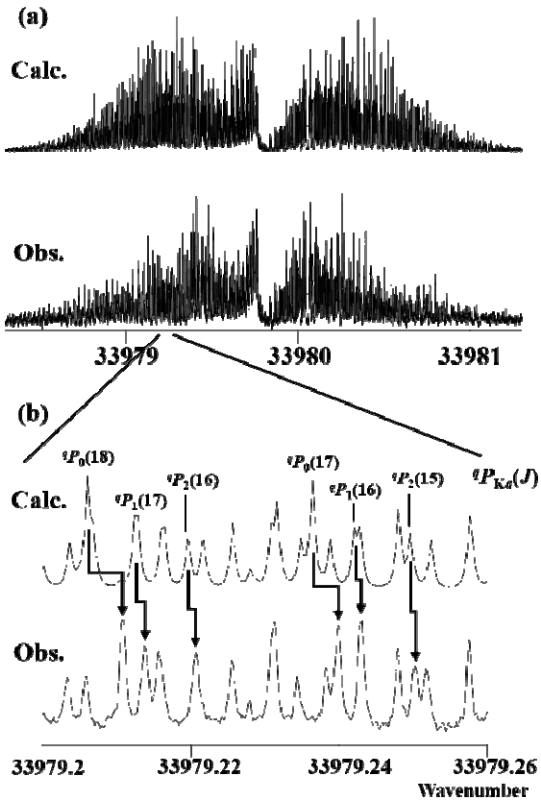

Figure 1. High-resolution spectra of the 0_0^0 + 204 cm^{-1} band. (a) is the whole spectra, (b) is the expanded spectra.

I-D. HIGH-RESOLUTION SPECTROSCOPY OF NO_2 AND NO_3 RADICAL

Doppler-free high-resolution spectroscopy was applied to investigate the electronic states of radicals. The radicals are very sensitive to the magnetic field because the spin quantum number is a half integer, it is expected to observe large Zeeman splitting even in the small magnetic field. The Zeeman splitting is very useful to assign the observed rotational lines even in the strong perturbing region. Nitrogen dioxide NO_2 and nitrate radical NO_3 have been known as an important intermediate in chemical reaction in the atmosphere. These radicals are the prototype molecules to understand vibronic interaction, and therefore these radicals become one of the model molecule for understanding the Renner-Teller effect for NO_2, and the Jahn-Teller (JT) and pseudo Jahn-Teller (PJT) effects for NO_3. The optically allowed transition has been observed as a strong absorption and LIF excitation spectrum by several groups. For NO_2 radical, hyperfine splittings are observed in high-resolution spectrum, and the amount of the hyperfine constants suggest the electronic excited state is mixed with the ground state through the vibronic interaction. For NO_3 radical, the strongest absorption line at 662 nm is called as 0-0 band of *B*-*X* transition which is used to detect the NO_3 radical in the atmosphere, however, the rotational assignment still remained because it is too complicated. Recently, we

reported the rotationally-resolved high-resolution spectrum and the Zeeman splittings of the 0-0 band of the *B-X* transition by using Doppler-free high-resolution spectroscopic technique.

Hyperfine interaction constants of $^{14}NO_2$ in 14500-16800 cm^{-1} region

Kohei Tada[1], Michihiro Hirata, and Shunji Kasahara[2]

[1]Kyoto University

(*J. Chem. Phys. 2017*)

We observed hyperfine-resolved high-resolution fluorescence excitation spectra of $k = 0$, $N = 1 \leftarrow 0$ transitions in 82 vibronic bands of the $A^2B_2 \leftarrow X\ ^2A_1$ system of $^{14}NO_2$ in the 14500–16800 cm^{-1} region by crossing a jet-cooled molecular beam and a single-mode dye laser beam at right angles. We determined hyperfine interaction constants of the lower and upper states for all the observed vibronic bands based on the analysis of the hyperfine structures of $k = 0$, $N = 1 \leftarrow 0$ transitions. Most of the determined Fermi contact interaction constants were found to be distributed in 0.0013–0.0038 cm^{-1}, which are intermediate in magnitude between those in lower and higher energy region reported by other groups. A sharp decreasing of the Fermi contact interaction constant was found in 16200–16600 cm^{-1}, and it may be caused by the interaction with the dark C $^2A_2$ state. The hyperfine interaction constants are powerful clues to obtain reliable vibronic assignment. We tentatively assigned vibronic bands located at 14836 cm^{-1}, 15586 cm^{-1}, and 16322 cm^{-1} as the transitions to the intrinsic (0,7,0), (0,8,0), and (0,9,0) vibrational levels of the A^2B_2 state, respectively.

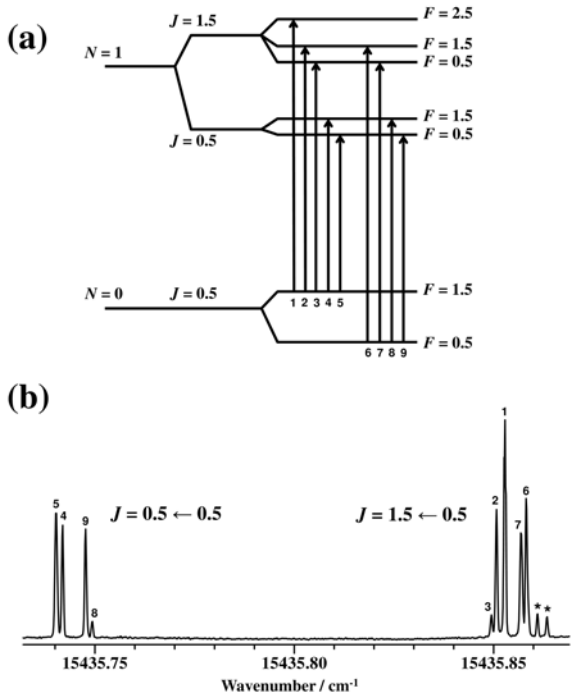

Figure 1. (a) The transition scheme among the hyperfine levels in the *R*(0) transition in the *J*-coupling scheme. (b) The observed hyperfine structure of the *R*(0) transition located at 15435.8 cm^{-1}. The signals with asterisks are other hyperfine lines.

Rotationally-Resolved High-Resolution Laser Spectroscopy of *B-X* transition of Nitrate Radical

Shunji Kasahara, Kohei Tada, Michihiro Hirata, Takashi Ishiwata[1], and Eizi Hirota[2]

[1]Hiroshima City University

[2]The Graduate University for Advanced Studies

(*34th International Symposium on Free Radicals, 2017*)

The nitrate radical NO_3 has been known as an

important intermediate in chemical reaction in the night-time atmosphere. The three lowest electronic states $X\ ^2A_2$', $A\ ^2E$'', and $B\ ^2E$' are coupled by vibronic interaction, and therefore NO_3 radical becomes one of the model molecule for understanding the Jahn-Teller (JT) and pseudo Jahn-Teller (PJT) effects. The optically allowed *B*-*X* transition has been observed as a strong absorption and LIF excitation spectrum by several groups. The strongest absorption line at 662 nm is called as 0-0 band of *B*-*X* transition which is used to detect the NO_3 radical in the atmosphere, however, the rotational assignment still remained because it is too complicated. [1] Recently, we reported the rotationally-resolved high-resolution spectrum and the Zeeman splittings of the *B*-*X* 0-0 band for $^{14}NO_3$ [2, 3] and $^{15}NO_3$ [4] by using sub-Doppler high-resolution spectroscopic technique. For NO_3 radical, it is expected to observe large Zeeman splitting even in the small magnetic field. The Zeeman splitting is very useful to assign the observed rotational lines even in the strong perturbing region. We expanded the measurement of the transition to vibrationally excited state observed around 628 nm.

NO_3 was produced by a pyrolysis reaction of N_2O_5 at 300ºC ($N_2O_5 \rightarrow NO_3 + NO_2$) with a heater attached to a pulsed nozzle, and collimated to a molecular beam with a skimmer and a slit. Rotationally - resolved high-resolution fluorescence excitation spectra were measured by crossing a single-mode laser beam perpendicular to a collimated NO_3 beam. The typical linewidth was 30 MHz and the absolute wavenumber was calibrated with accuracy 0.0001 cm^{-1} by measurement of the Doppler-free saturation spectrum of iodine molecule and fringe pattern of the stabilized etalon. The observed rotational lines were too complicated to find any rotational series. In the observed spectra, mainly the rotational line pairs from the $X\ ^2A_2$'(v''=0, K''=0, N''=1, F_1 and F_2 levels) are assigned unambiguously by using the combination differences of the $X\ ^2A_2$' state and measurement of the Zeeman splittings. The observed results suggest the observed vibrationally excited states of the $B\ ^2E$' state are also interacts with the other vibronic levels similar to the $B\ ^2E$'(υ'=0) level.

[1] R. T. Carter, K. F. Schmidt, H. Bitto, and J. R. Huber, *Chem. Phys. Lett.* **257**, 297 (1996).

[2] K. Tada, W. Kashihara, M. Baba, T. Ishiwata, E. Hirota, and S. Kasahara, *J. Chem. Phys*. **141**, 184307 (2014).

[3] K. Tada, T. Ishiwata, E. Hirota, and S. Kasahara, *J. Mol. Spectrosc*., **321**, 23 (2016).

[4] K. Tada, K. Teramoto, T. Ishiwata, E. Hirota, and S. Kasahara, *J. Chem. Phys.* **142**, 114302 (2015).

II. Terahertz Molecular Chemistry Laboratory

II-A. LIQUID DYNAMICS STUDIED BY NONLINEAR INFRARED SPECTROSCOPY

Molecular dynamics in liquids are strongly affected by the nature of intermolecular interactions. It is greatly important to obtain the molecular description on relation between the dynamics and interactions in liquids in order to elucidate the solvent dynamical effect on chemical reactions. Fluctuations of the vibrational transition energies, which are characterized by time correlation functions of the frequency fluctuations, are very sensitive to the dynamics of surrounding environments. Vibrational energy relaxation is also affected by short-range solvent-oscillator interaction. Furthermore, orientational relaxation reflects microscopic viscosity around the oscillator. In recent years, a great deal of effort has been devoted to investigate solute-solvent interactions with infrared (IR) nonlinear spectroscopy. The vibrational frequency fluctuations can be investigated by three-pulse photon echo and two-dimensional IR spectroscopy. By polarization-sensitive pump-probe spectroscopy in the IR region we can study vibrational energy relaxation and orientational relaxation.

Rotational Dynamics of Solutes with Multiple Single Bond Axes Studied by Infrared Pump-Probe Spectroscopy

Masaki Okuda, Kaoru Ohta, and Keisuke Tominaga

(*J. Phys. Chem. B 2017*)

To investigate the relationship between the structural degrees of freedom around a vibrational probe and the rotational relaxation process of a solute in solution, we studied the anisotropy decays of three different N_3-derivatized amino acids in primary alcohol solutions. By performing polarization-controlled IR pump-probe measurements, we reveal that the anisotropy decays of the vibrational probe molecules in 1-alcohol solutions possess two decay components, at sub-picosecond and picosecond time scales. Based on results showing that the fast relaxation component is insensitive to the vibrational probe molecule, we suggest that the anisotropy decay of the N_3 group on a sub-picosecond time scale results from a local, small-amplitude fluctuation of the flexible vibrational probe, which does not depend on the details of its molecular structure. On the other hand, the slow relaxation component depends on the solute: with longer alkyl chains attached to the N_3 group, the anisotropy decay of the slow component is faster. Consequently, we conclude that the slow relaxation component corresponds to the reorientational motion of the N_3 group correlated with other intramolecular rotational motions (*e.g.,* rotational motions of the neighboring alkyl chain). Our experimental results provide important insight into understanding the rotational dynamics of solutes with multiple single bond axes in solution.

Theoretical investigation on vibrational frequency fluctuations of SCN-derivatized vibrational probe molecule in water

Masaki Okuda, Masahiro Higashi[1], Kaoru Ohta, Shinji Saito[2], and Keisuke Tominaga

[1]Univeristy of the Ryukyus

[2]Institute for Molecular Science

(*Chem. Phys. 2018*)

In order to establish a molecular picture on the vibrational frequency fluctuations of SCN stretching mode of 2-nitro-5-thiocyanate benzoic acid (NTBA) in H_2O, we theoretically investigated the structural fluctuations of the local environment around the solute by using the classical MD simulations. By calculating the solute-solvent pair radial distribution function, the hydrogen-bond correlation function, and the single-water dipole moment correlation function, we elucidated that the hydration structure and water dynamics in the vicinity of the SCN group of NTBA are almost similar to those in bulk. Moreover, by calculating the spatially-resolved frequency-frequency time correlation function (FFTCF) and the electrostatic potential on the vibrational probe, we revealed that longer-range solute-solvent interaction is important for the SCN vibrational frequency fluctuations of NTBA, which is a different result from our previous work for SCN^-/water system [1]. Therefore, we consider that the electrostatic interactions with such "bulk-like" water molecules are responsible for the slow decay component (*i.e.* 1-ps decay component) of the FFTCF of NTBA in H_2O. This is in a sharp contrast with the molecular mechanism for the FFTCF of SCN^- in H_2O, where the SCN vibrational frequency fluctuations are controlled by the water molecules tightly hydrogen bonding to the ion. Therefore, from the comparison between our current and previous studies, it is suggested that the molecular origin of vibrational frequency fluctuations can be significantly different between ionic and non-ionic vibrational probe molecules in terms of the solute-solvent interactions and solvation dynamics, even if we observe similar time scales of decay components in their FFTCFs by 2D-IR spectroscopy.

[1] M. Okuda, M. Higashi, K. Ohta, S. Saito, and K. Tominaga, *Chem. Phys. Lett.* **683**, 547-552 (2017)

Hydrogen-bond dynamics of 9-fluorenone derivatives in water probed by 2D-IR spectroscopy

M. Okuda, K. Ohta, and K. Tominaga

(*TRVS 2017*)

In aqueous solution, hydrogen bond (HB) between solute and solvent molecules strongly perturbs the dynamic and static properties of the solute molecules, which affects the reactivity of chemical reaction in solution. Vibrational frequency is well-known to be sensitive to the environmental change around solute molecules in solution. Two-dimensional infrared (2D-IR) spectroscopy is a powerful tool to quantify the vibrational frequency fluctuation of solute molecules, which results from the temporal fluctuation in solute-solvent interaction on an ultrafast time scale (sub-ps ~ ps time scale).

In this study, by using 2D-IR spectroscopy, we have investigated the vibrational frequency fluctuations of two different 9-fluorenone derivatives (9-FL-2-COO^- and 9-FL-4-COO^-) in

D_2O. As shown in Figure 1(a), the IR spectrum of 9-FL-2-COO^- in D_2O exhibits the asymmetric lineshape, which likely results from two different types of solute-water HB complexes [1]. Figure 1(b) shows the 2D-IR spectrum of 9-FL-2-COO^- in D_2O measured at population time (T) of 0 ps. We found that the relative amplitude of the cross peak (S_{AB}) to the diagonal peak signals (S_{AA}) becomes larger with population time T (see Figure 1(c)), which reflects the making and breaking of a HB between 9-FL-2-COO^- and a water molecule. On the other hand, the 2D-IR spectra of 9-FL-4-COO^- in D_2O show no cross peak signals. Based on these 2D-IR results, we conclude that the position of the COO^- group plays an important role for the solute-water HB dynamics.

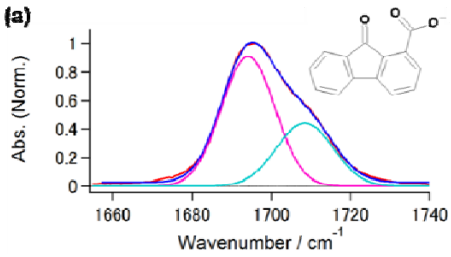

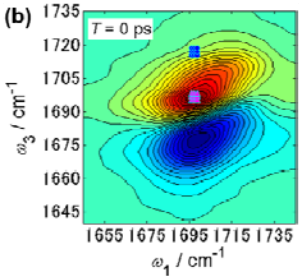

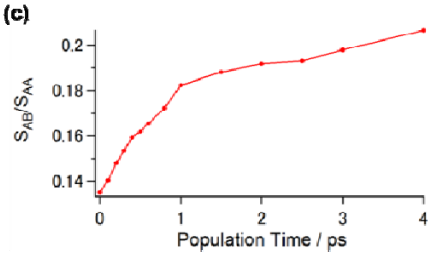

Figure 1. (a) IR spectrum of the carbonyl CO stretching mode of 9-FL-2-COO^- in D_2O. Molecular structure of 9-FL-2-COO^- is shown in the right-top. (b) 2D-IR spectrum of 9-FL-2-COO^- in D_2O measured at T = 0 ps. Closed circles and triangles indicate areas of integration used to determine the S_{AA} (pink) and S_{AB} (blue), respectively. (c) temporal profile of the S_{AB}/S_{AA} as a function of population time.

[1] S. Hirai *et al.*, *Chem. Phys. Lett.*, **450**, 44−48 (2007).

II-B. DYNAMICS OF ELECTRONICALLY EXCITED STATE IN CONDENSED PHASES

Understanding of dynamics in the electronically excited state is a key issue to elucidate mechanisms in various photochemical reactions in condensed phases. It is also important for designing and developing new materials which have characteristic functions. We employ various kinds of ultrafast technique to monitor photochemical and photophysical invents in sub-pico- to picoseconds time scales. By femtosecond fluorescence up-conversion technique, dynamics in the electronically excited state can be observed with a time resolution up to 100 fs. Vibrational dynamics in the electronically excited can be investigate by UV/VIS-pump IR probe technique. Moreover, low-frequency responses by photoexcitation are investigated by UV/VIS-pump THz probe experiment. Such responses include change of low-frequency vibrational modes induced by photoexcitation and photo-induced changes of charge carrier dynamics.

Charge carrier dynamics of GaAs/AlGaAs asymmetric double quantum wells at room temperature studied by optical pump terahertz probe spectroscopy

Jessica Afalla, Kaoru Ohta, Shunrou Tokonami, Elizabeth Ann Prieto[1], Gerald Angelo Catindig[1], Karl Cedric Gonzales[1], Rafael Jaculbia[1], John Daniel Vasquez[1], Armando Somintac[1], Arnel Salvador[1], Elmer Estacio[1], Masahiko Tani[2], and Keisuke Tominaga

[1]*University of the Philippines Diliman*

[2]*University of Fukui*

(*Jpn. J. Appl. Phys. 2017*)

Two asymmetric double quantum wells of different coupling strengths (barrier widths) were grown via molecular beam epitaxy, both samples allowing tunneling. Photoluminescence was measured at 10 and 300 K to provide evidence of tunneling, barrier dependence and structural uniformity. Carrier dynamics at room temperature was investigated by optical pump terahertz probe (OPTP) spectroscopy. Carrier population decay rates were obtained and photoconductivity spectra were analyzed using the Drude model. This work demonstrates that carrier and possibly tunneling dynamics in asymmetric double quantum well structures may be studied at room temperature through OPTP spectroscopy.

Probing Charge Carrier Dynamics in Porphyrin-based Organic Semiconductor Thin Films by Time-resolved THz Spectroscopy

Kaoru Ohta, Shunrou Tokonami, Kotaro Takahashi[1], Yuto Tamura[1], Hiroko Yamada[1] and Keisuke Tominaga

[1]Nara Institute of Science and Technology

(J. Phys. Chem. B 2017)

To improve the power conversion efficiency of solar cells, it is important to understand the underlying relaxation mechanisms of photogenerated charge carriers in organic semiconductors. In this work, we studied the charge carrier dynamics of diketopyrrolopyrrole-linked tetrabenzoporphyrin thin films where the diketopyrrolopyrrole unit has two *n*-butyl groups, abbreviated as C4-DPP-BP. We used time-resolved terahertz (THz) spectroscopy to track charge carrier dynamics with excitations at 800 nm and 400 nm. Compared with tetrabenzoporphyrin (BP), the extension of π-electron delocalization to the diketopyrrolopyrrole peripherals leads to an increase in absorption in the near-infrared region. Following the excitation at 800 nm, we found that the transient THz signals in C4-DPP-BP thin films decay with time constants of 0.5 ps and 9.1 ps, with small residual components. With the excitation at 400 nm, we found that the transient THz signals decay with time constants of 0.4 ps and 7.5 ps. Based on the similarity of the decay profiles of the transient THz signals obtained with excitations at 400 nm and 800 nm, we considered that the decaying components are due to charge carrier recombination and/or trapping at defect sites, which do not depend on the excess energy of the photoexcitation. In contrast to BP, even without an electron acceptor, we observed the finite offset of the transient THz signals at 100 ps, demonstrating the existence of long-lived charge carriers. We also measured the photoconductivity spectra of C4-DPP-BP thin films with the excitation at both 800 nm and 400 nm. It was found that the spectra

can be fitted by the Drude–Smith model. From these results, it was determined that the charge carriers are localized right after photoexcitation. At 0.4 ps, the product of the quantum yield of charge generation and mobility of charge carriers at 400 nm is approximately twice that obtained at 800 nm. We discuss the implications of the excess excitation energy in organic semiconductor-based devices.

II-C. MOLECULAR DYNAMICS IN THE TERAHERTZ FREQUENCY REGION IN CONDENSED PHASES

Vibrational spectroscopy has been widely used to investigate structures, interactions and dynamics of molecules and molecular complexes. The low-frequency region below several terahertz (THz; 1 THz = 33.3 cm^{-1}) corresponds to intermolecular modes of complexes and intramolecular modes with a weaker potential force and/or larger reduced mass. Intermolecular interactions such as hydrogen bonding, van der Waals forces and charge-transfer interactions play important roles in various chemical and biological processes. Moreover, the low-frequency spectra also reflect molecular dynamics on a time scale from picoseconds to femtoseconds. There has been dramatic progress in the generation and detection techniques of freely propagating THz radiation in the past two decades. The examples of the generation technique include photoconductive switching, optical rectification, and the surface photocurrent of semiconductors. Because the pulse duration of the THz radiation is in a sub-picosecond time region, it is possible to measure the electric field of the radiation by coherent detection methods, which consequently allows us to conduct THz time-domain spectroscopy (TDS). By THz-TDS we can obtain the refractive index and extinction coefficient of a medium by measuring the phase and amplitude of the radiation. THz-TDS is an attractive method for studying dynamics in condensed phases with time scales of sub-picoseconds and picoseconds. We have applied THz-TDS to investigate various kinds of condensed materials, including neat liquids and mixtures of liquids, biological polymers, and charge carrier dynamics in semiconductors and conducting polymers.

Effect of Temperature and Hydration Level on Purple Membrane Dynamics Studied Using Broadband Dielectric Spectroscopy from Sub-GHz to THz Regions

Naoki Yamamoto[1], Shota Ito[2], Masahiro Nakanishi[3], Eri Chatani[1], Keiichi Inoue[2], Hideki Kandori[2], Keisuke Tominaga

[1]Graduate School of Science, Kobe University

[2]Nagoya Institute of Technology

[3]Fukuoka Institute of Technology

(*J. Phys. Chem. B, 2018*)

To investigate the effects of temperature and hydration on the dynamics of purple membrane (PM), we measured the broadband complex dielectric spectra from 0.5 GHz to 2.3 THz using a vector network analyzer and terahertz time-domain spectroscopy from 233 to 293 K. In the lower temperature region down to 83 K, the complex dielectric spectra in the THz region were also obtained. The complex dielectric spectra were

analyzed through curve fitting using several model functions. We found that the hydrated states of one relaxational mode, which was assigned as the coupled motion of water molecules with the PM surface, began to overlap with the THz region at approximately 230 K. On the other hand, the relaxational mode was not observed for the dehydrated state. Based on this result, we conclude that the protein-dynamical-transition-like behavior in the THz region is due to the onset of the overlap of the relaxational mode with the THz region. Temperature hysteresis was observed in the dielectric spectrum at 263 K when the hydration level was high. It is suggested that the hydration water behaves similarly to super-cooled liquid at that temperature. The third hydration layer may be partly formed to observe such a phenomenon. We also found that the relaxation time is slower than that of a globular protein, lysozyme and the microscopic environment in the vicinity of the PM surface is suggested to be more heterogeneous than lysozyme. It is proposed that the spectral overlap of the relaxational mode and the low-frequency vibrational mode is necessary for the large conformational change of protein.

Terahertz Spectroscopy and Theoretical Calculation on Biologically Important Molecules and Pharmaceutical Molecules

Feng Zhang, Hong-Wei Wang[1], Michitoshi Hayashi[1], Tetsuo Sasaki[2], and Keisuke Tominaga

[1]National Taiwan University

[2]Shizuoka University

(*2nd International Symposium on Biomedical Engineering 2017*)

THz techniques have been mature thanks to the continuous advances in the past two decades. At present, the community desires to seek any ubiquitous application grounds of THz spectroscopy where other analysis methods are incompetent. To this end, we would like to emphasis the necessity of quantitative theoretical interpretation. The philosophy is simple—breakthrough applications of any spectroscopic method emerge only after we understand the real nature of the signals we desire to use. In this work, we intend to show how the interplay of terahertz spectroscopy and solid-state density functional theory (DFT) sheds a quantitative light on THz motions. We use two systems—biomolecules and pharmaceuticals, which attract great interest, for the illustration.

Figure 1 compares the experiment and theory for a set of biomolecular crystals including a monosaccharide, a disaccharide, and a short-chain peptide [1, 2]. Good and consistent agreements between experiment and theory are observed in all the systems, indicating the reliability and stability of the DFT method applied. On the basis of accuracy calculations, we characterized the nature of all the observed THz modes with using a quantitative mode-decomposition method recently developed [3, 4]. Normal modes in this region may have contributions under the harmonic approximation from both intermolecular and intramolecular nuclear motions. A newly developed mode analysis allows us to characterize molecular optical phonon modes in terms of intermolecular and intramolecular vibrational mixing. This method allows us to first decompose any molecular motion

of interest into a combination of intermolecular translations and librations, and a set of intramolecular vibrations with unambiguous physical meanings. We can then examine the percentage contributions of all the elemental vibrations to the potential energy of a certain THz modes in number. These analyses would enable us to examine the quantitative correlation between the nature of THz modes and various molecular properties, e.g. the chain-lengths of saccharides and peptides, and the packing structures of polymorphs.

[1] F. Zhang, et al., *J. Phys. Chem. A*, **2015**, 119, 3008-3022.

[2] F. Zhang, et al., *Chem. Asian J.*, **2017**, 12, 324-331.

[3] F. Zhang, et al., *J. Chem. Phys.*, **2014**, 140, 174509.

[4] F. Zhang, et al., *WIREs Comput. Mol. Sci.*, **2016**, 6, 386-409.

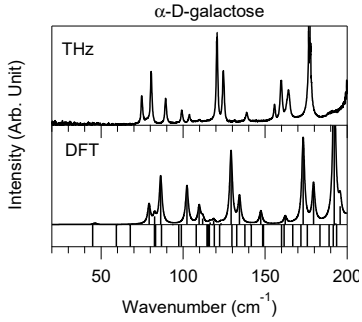

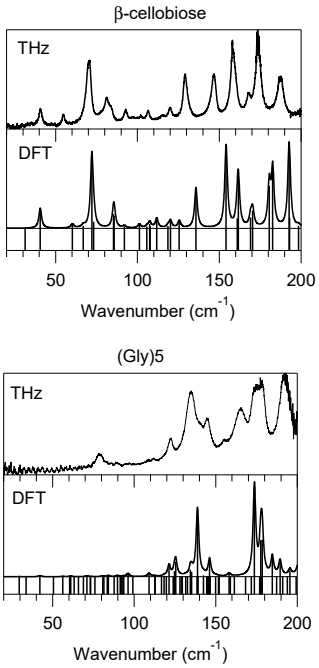

Figure 1. Comparison between THz spectra and DFT calculation results for a set of biomolecular systems. THz spectra were measured with a continuous THz-wave system and at 10 K. DFT calculations were performed in the CRYSTAL14 software package.

II-D. INTERMOLECULAR INTERACTIONS OF POLYMER STUDIED BY TERAHERTZ SPECTROSCOPY

THz spectroscopy is a powerful tool that uses the low frequency vibrational modes to elucidate the intermolecular interaction and the higher order structure of large molecules. We have investigated the inter- and intramolecular interactions of various kinds of polymers by THz spectroscopy, infrared (IR) spectroscopy, and quantum chemical calculations (QCCs). Since the physical properties of polymeric materials are closely correlated to the higher order structure such a lamellae structure, the investigation of higher-order structure helps to understand the physical properties of polymer directly.

Intermolecular Interaction and Higher-Order Structure of Biodegradable Polyester Studied by Terahertz Spectroscopy

Harumi Sato, Chihiro Funaki

(*9th International Conference on Advanced Vibrational Spectroscopy* (*ICAVS-9*))

In recent times, terahertz (THz) imaging has been a subject of considerable interest since this technique can be used to visualize the distribution of the different components in a nonhomogeneous material such as pharmaceutical tablets, semiconductor wafers, and biomedical subjects. THz spectroscopy is a powerful tool that uses the low frequency vibrational modes to elucidate the intermolecular interaction and the higher order structure of large molecules.[1-5] Hence, THz spectroscopy should provide valuable information towards understanding the origin of the higher order conformation in large molecules. In addition, THz imaging makes it possible to explore the higher order structure of a sample without altering or destroying it. In the present study, we have investigated the characterization of PCL by THz imaging.

In the THz spectra of crystalline PCL, two major peaks are observed at 1.6 and 2.2 THz.[6] It is known that PCL in its crystal structure has a planar zigzag molecular chain conformation. The peak at 2.2 THz has been assigned to the parallel mode to the stretching direction, and the peak at 1.6 THz has been attributed to the vibration due to the perpendicular mode by using polarized THz absorption at 10 K. By using these peaks and their intensity ratios, we have investigated distribution of both crystallinity and crystalline orientation in PCL films.

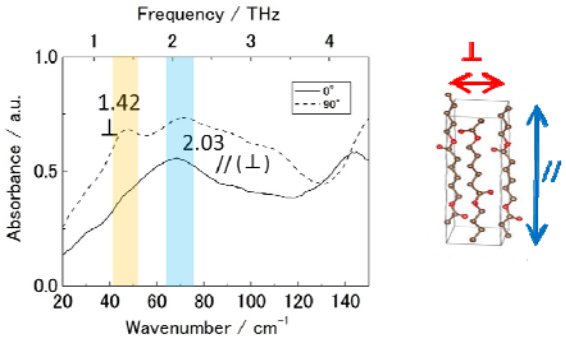

Figure 1. Polarized THz absorption spectra of a highly stretched PCL film. The angle between the stretched direction and the electric field of the THz wave was set to 0º (//) and 90 º (⊥).

Figure 2 shows the polarized THz images prepared by using the peak intensity at 1.42 THz of PCL press film of 90 º (⊥) and 0 º (//). The angle between a vertical line on the image and the electric field of the THz wave was set to 0 º and 90 º. The image developed by the intensity ratio $I_{1.42}$ (90 º)/$I_{1.42}$ (0 º) is shown in Figure 2.

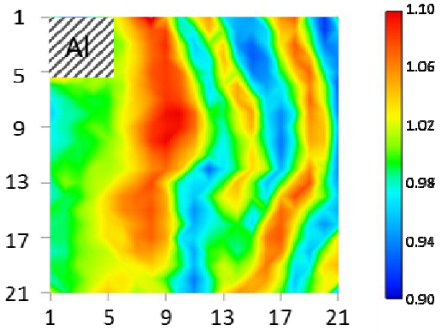

Figure 2. The THz image of a PCL film based on the intensity ratio of I1.42 at 90 º (⊥) and that at 0 º (//). The angle between vertical line on the image and the electric field of the THz wave was set to 0 º and 90 º. The THz imaging measurement was carried out by putting the aluminum tape to the upper-left corner to fix the measurement position.

If there are some polarization properties in the PCL hot-pressed film, the image should show some sort of pattern. This THz image indicates the crystalline orientation of the PCL film. These stripe patterns suggest that the crystalline orientation occurs because polymer chains are stretched and crystallized during the film preparation. It is clearly shown that the THz imaging reveals the crystalline orientation of the polymer.

[1] H. Hoshina et al. *Phys. Chem. Chem. Phys*. **2011**, 13(20), 9173–9179.
[2] H. Hoshina et al. *Appl. Phys. Lett.* **2012**. 100(1), 011907.
[3] H. Hoshina et al. *Appl. Phys. Lett.* **2010**. 96(10), 101904.
[4] H. Hoshina et al. *IEEE Trans. Terahertz Sci. Technol.* **2013**. 3(3), 248–258.
[5] H. Suzuki et al. *Chem. Phys. Lett*. **2013**. 575: 36–39.
[6] M. Komatsu et al. *J. Appl. Phys.* **2015**. 117(13), 133102.

Thermal Denaturation and structural changes of collagen model peptide studied by low frequency Raman and THz spectroscopy

Tomoki Nagahama, Harumi Sato

(*9th International Conference on Advanced Vibrational Spectroscopy (ICAVS-9)*)

Collagen is protein that occupies about 30% of all proteins contained in body and it plays important role to sustain the function of body. Collagen has been used as not only cosmetics or health food but also medical materials like vascular grafts, smoothing wrinkle on skin, contact lenses, cover materials used when you get burned. However, the studies about the investigation of function of collagen particularly interaction with protein have not been advanced. In this study, we tried to investigate the triple helical structure changes of collagen by low frequency Raman and terahertz (THz) spectroscopy. We focused on the low frequency region which reflects higher order structure of polymer.

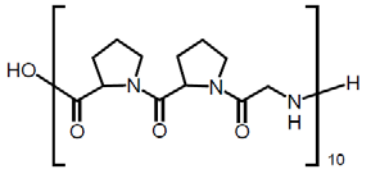

Figure 1 Chemical structure of PPG10.

The sample used for experiments were collagen model peptide ((Pro-Pro-Gly)$_{10}$; PPG10, Peptide institute, Inc., denaturation temperature(Td) = 30^{o}C; Figure 1). In this study, PPG10 were used as is (powder condition) or dissolved in D_2O. PPG10 of powder and solution were measured by low frequency Raman at room temperature or getting up or down temperature used by temperature controller, T95-HS (LINKAM Scientific Instruments). Low frequency Raman spectra were measured by SureBlock XLF-CLM (ONDAX, Inc., resolution: 3.5cm^{-1}, excitation wavelength: 830 nm, Exposure time: 1s, No. of averaging: 50 times, transmittance: 20-1590 cm^{-1}) and HR-800-LWR (HORIBA, Ltd., resolution: 1 cm^{-1}, excitation wavelength: 514.5 nm, Exposure time: 5s, No. of scan: 20 times, transmittance: 70-3200 cm^{-1}) spectrometers.

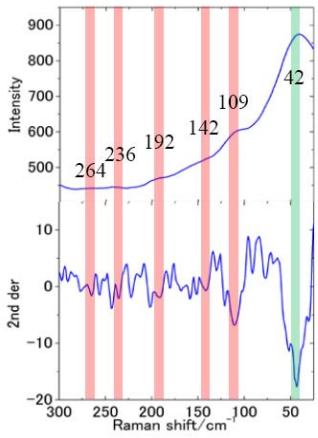

Figure 2 Low frequency Raman spectrum and its second derivative of PPG10 powder.

Low frequency Raman spectrum and its second derivative at room temperature of PPG10 are shown in Figure 2. There were several peaks (42 cm^{-1}, 109cm^{-1}, 142 cm^{-1}, 192 cm^{-1}, 236 cm^{-1}, 264cm^{-1}) in the region of 300 cm^{-1} or less. Moreover, in the region of 300 cm^{-1} or more, the peak in spectrum coincided with preceding study.[1] It was revealed by FT-IR (Fourier Transform Infrared) that PPG10 (1wt%, dissolved in D_2O) formed triple helix structure at room temperature (25 ºC) and denatured at high temperature (60 ºC). Figure 3 shows the low frequency Raman spectra of PPG10 solution at room temperature (25 ºC) and high temperature (50 ºC).

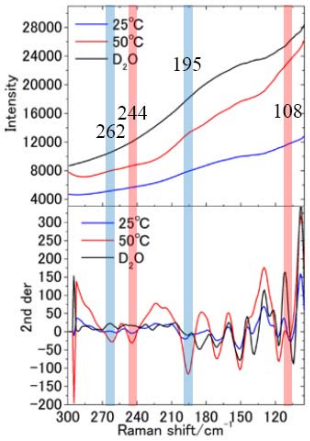

Figure 3. Low frequency Raman spectra and theirs second derivative of PPG10 solution and D_2O.

The Raman spectrum in the low frequency region at 50 ºC which is denatured triple helical structure is slightly different from that of Raman spectrum at 25 ºC. We are trying to assign the peak derived from triple helix structure by measuring PPG10 solution with a thick consistency or collagen sheet by THz spectroscopy.

[1] A. Merlino et al. *Biophysical Chemistry* **2008**, 137(1), 24–27.

Low-Frequency Vibrational Modes of Crystalline Polyesters and Interchain Interaction Studied by Using DFT Calculation

Shigeki Yamamoto[1], Harumi Sato, Hiromichi Hoshina[2], Yukihiro Ozaki[3]

[1]Osaka University

[2]RIKEN

[3]Kwansei Gakuin University

(*9th International Conference on Advanced Vibrational Spectroscopy (ICAVS-9)*)

Insight into higher-order structures and intermolecular interactions of crystalline polymer chains can be achieved by using low-frequency Raman, far infrared (FIR), and terahertz time-domain (THz-TD) spectroscopies. However, the spectral interpretation has been limited so far owing to still uncertain assignments of the modes. A fragment-based quantum mechanical calculation, the Cartesian-coordinate tensor transfer,[1,2] can simulate the spectra of large molecular systems with

acceptable accuracy and realistic calculation time, as shown in our works on poly(glycolic acid) (PGA)[3] and poly-(R)-hydroxybutyrate (PHB).[4] For both crystalline polyesters, good agreements were achieved between the experiments and theories in both Raman and FIR/THz-TD spectra. The DFT-based assignments enabled us to interpret the spectral change in relation to the higher-order structures/intermolecular interactions. In the case of PGA, the simplest aliphatic polyester with a lamellar zigzag crystal structure, the measured spectra down to 50 cm^{-1} were compared with the calculated spectra (Figure 1)[3]. The low-frequency bands were assigned on the basis of agreements found in polarization directions and spectral shapes of both Raman and FIR spectra. Temperature dependence of the experimental spectra clarified that only the bands at 70 cm^{-1} in FIR and 125 cm^{-1} in Raman shifted to the lower-frequency with increasing temperature. The thermally-shifted bands were assigned to interchain modes composed of out-of-plane bending motion of C=O groups and rocking/twisting of CH_2 groups. The origin of the thermal shift was examined by the spectral calculation and natural bond orbital (NBO) analysis and clarified that it was caused by thermal expansion of crystal lattice and succeeding changes in orbital interactions between C=O and CH_2 groups among the polymer chains. Lamellar crystalline PHB has been considered to include weak hydrogen bonds between C=O and CH_3 groups among the polymer chains.[5]

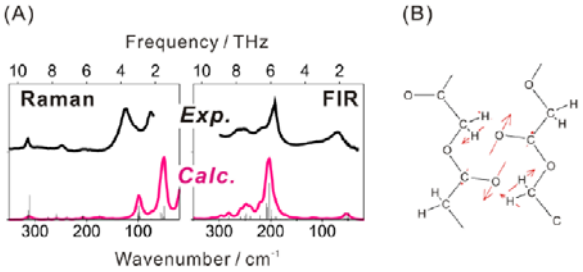

Figure 1. (A) Comparisons of experiments (black lines) and theories (red lines) of FIR and Raman spectra of crystalline PGA (B) calculated main atomic motion of the Ramanactive and temperature-sensitive band experimentally observed at 125 cm^{-1} . The theory used: CAM-B3LYP-GD3BJ /6-311++G** with a fragment methodology.[3]

The calcualted Raman and FIR spectra with an explicit consideration of the interchain interactions gave good agreements with the experiments in terms of spectral shapes, frequencies, and intensities (Figure 2)[4]. The calculation explored that a strong experimental Raman band at 79 cm^{-1} comes from the intermolecular vibrational mode of the out-of-plane C=O+CH_3 vibration, which would directly reflect the proposed interchain hydrogen bonds.

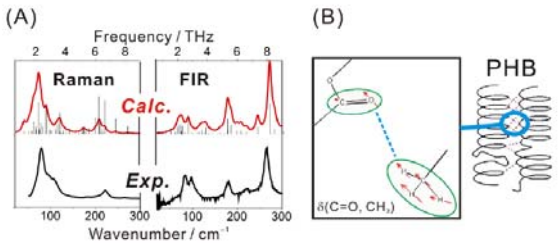

Figure 2. (A) Comparisons of experiment (black lines) and theory (red lines) of Raman and FIR spectra of crystalline PHB (B) calculated main atomic motion of the Raman active band experimentally observed at 79 cm^{-1} . The theory used: B97-1/6-31++G** with a fragment methodology.[4]

[1] P. Bouř et al. *J. Comput. Chem*. **1997**, *18*, 646−659.

[2] S. Yamamoto et al. *J. Chem. Theory Comput.* **2012**, *8,* 977-985.

[3] S. Yamamoto et al. *J. Phys. Chem. B* **2017**, *121*, 1128-1138.

[4] S. Yamamoto et al. *J. Phys. Chem. B* **2013**, *117,* 2180-2187.

[5] H. Sato et al. *Macromolecules* **2008**, *41*, 4305-4312.

Intermolecular interactions of poly(3-hydroxybutyrate-co-3-hydroxyvalerate) (P(HB-*co*-HV)) with PHB-type crystal structure and PHV-type crystal structure studied by low-frequency Raman and terahertz spectroscopy

Dian Marlina,[1] Harumi Sato, Hiromichi Hoshina,[2] Yukihiro Ozaki[1]

[1]Kwansei Gakuin University

[2]RIKEN

(*Polymer*, **135**, 331-337 (2018))

Composition-, temperature-, and polarization-dependent low-frequency Raman and terahertz (far-infrared; FIR) spectra were measured for poly(3-hydroxybutyrate-*co*-3-hydroxyvalerate) (P(HB-*co*-HV); Fig.1) with PHB-type crystal structure and PHV-type crystal structure to investigate their intermolecular interactions. Band assignments were attempted by comparing the low-frequency Raman (Fig.2) and terahertz (FIR) spectra (Fig.3) of P(HB-*co*-HV) with the varying HV content with the corresponding spectra of PHB and by observing spectral variations.

The spectra of P(HB-*co*-HV) (HV = 9, 15, and 21 mol %) are similar to the corresponding spectra of PHB. There are two bands at 97 and 82 cm^{-1} which are assigned to a spring type vibrational mode of the helical structure and to the mode reflecting the intermolecular interaction (C-H···O=C hydrogen bond), respectively.

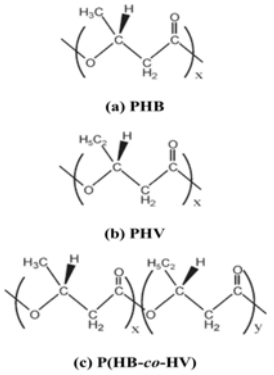

Figure 1. Chemical structures of (a) poly(3-hydroxybutyrate) (PHB), (b) poly(3-hydroxyvalerate) (PHV), and (c) poly(3-hydroxybutyrate-*co*-3-hydroxyvalerate) (P(HB-co-HV)).

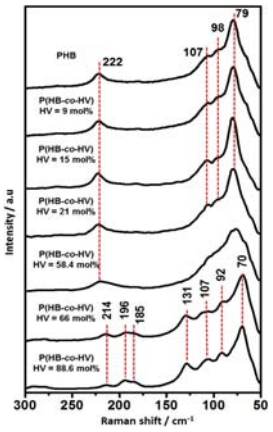

Figure 2. Low-frequency Raman spectra of PHB and P(HB-*co*-HV) with varying HV content.

The low-frequency Raman and terahertz spectra of P(HB-*co*-HV) with HV content of 66 and 88.6 mol% show bands at 91 and 78 cm^{-1}. The

78 cm^{-1} band is assigned to the intermolecular interaction (C-H···O=C hydrogen bond). In contrast to the 97 cm^{-1} band of P(HB-*co*-HV) with the low HV content, the 91 cm^{-1} band of P(HB-*co*-HV) with the high HV content show a temperature-dependent shift by 4 cm^{-1}. Thus, although it seems that both 97 and 91 cm^{-1} bands are due to spring-like vibrational modes, the nature of two vibrational modes seems to be significantly different, reflecting the difference in the intermolecular interaction.

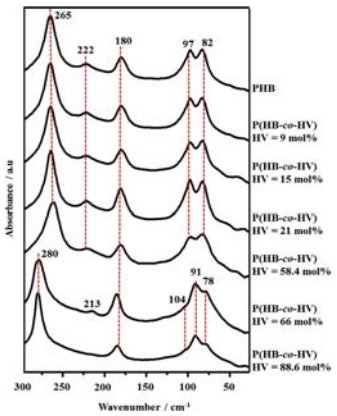

Figure 3. FIR spectra of PHB and P(HB-*co*-HV) with varying HV content.

Stress-induced crystal transition of poly(butylene succinate) studied by terahertz and low-frequency Raman spectroscopy and quantum chemical calculation

Seika Tatsuoka, Harumi Sato

(*Spectrochimica Acta* Part A (2018))

We measured terahertz (THz) and low-frequency Raman spectra of Poly (butylene succinate) (PBS) which shows the crystal transition from α to β by stretching. For the assignment of the absorption peaks in the low-frequency region, we performed quantum chemical calculations with Cartesian-coordinate tensor transfer (CCT) method. Four major peaks appeared in the THz spectra of PBS at around 58, 76, 90, and 100cm^{-1}, and in the low-frequency Raman spectra a peak was observed at 88cm^{-1}. The THz peak at 100cm^{-1} and the Raman peak at 88cm^{-1} show a shift to a lower wavenumber region with increasing temperature. The quantum chemical calculation of β crystal form reveals the new peak appears above 100cm^{-1}. It was found that two kinds of peaks overlapped at around 100cm^{-1} in the THz spectra of PBS. One of them can be assigned to a weak hydrogen bond between the C=O and CH_2 groups in the intermolecular chains, which is perpendicular to the molecular chain of the α crystal form. Another one showed a parallel polarization which can be assigned to the intramolecular interaction between O (ether) and H-C groups in the β crystal form. The position of the peak at around 100cm^{-1} in the perpendicular polarization changed to a lower wavenumber region with stretching, because of the weakening of the intermolecular hydrogen bonding by increasing the interatomic distances. On the other hand, that of the parallel polarization shifts to a higher wavenumber region because of the shortening of the interatomic distance from α to β crystal form (the strength of the intramolecular hydrogen bonding became stronger) by stretching.

Three different kinds of weak C-H···O=C inter- and intramolecular interactions in poly(ε-caprolactone) studied by using terahertz spectroscopy, infrared spectroscopy and

quantum chemical calculations

Chihiro Funaki, Shigeki Yamamoto[1], Hiromichi Hoshina[2], Yukihiro Ozaki[3], and Harumi Sato

[1] Osaka University

[2] RIKEN

[3] Kwansei Gakuin University

(*Polymer, 2017*)

The long range structure of poly(ε-caprolactone) (PCL; Fig.1) has been studied by terahertz (THz) spectroscopy, infrared (IR) spectroscopy and quantum chemical calculations (QCCs). Natural bond orbital (NBO) analysis and the calculation of the interatomic distances between C-H and O.C groups in PCL crystalline indicate that the PCL chain has three kinds of weak intermolecular interactions between the CH_2 and C=O groups.

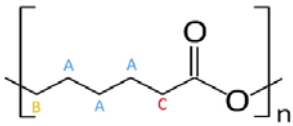

Figure 1. Chemical structure of poly(ε-caprolactone) (PCL). Pattern A: the CH_2 adjacent to methylene groups; pattern B: the CH_2 adjacent to ester groups; and pattern C: the CH_2 adjacent to carbonyl groups.

In the IR spectra, significant changes due to the influence of hydrogen bondings were observed in the CH_2 and C=O stretching vibration regions. The results of QCCs performed by using the Cartesian Coordinate Tensor Transfer (CCT) method to assign the THz spectra of PCL suggest that the peaks at 47 and 67 cm^{-1} reflect the atomic motions of the C=O + CH_2 moiety derived from the weak C-H···O=C hydrogen bondings.

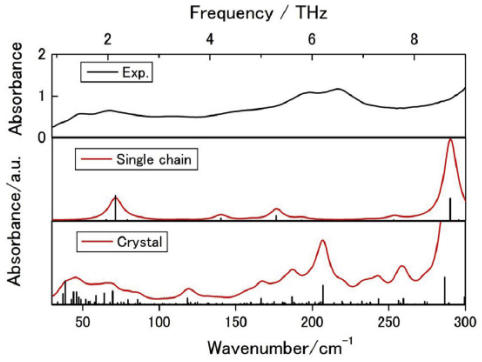

Figure 2. Experimental spectrum of PCL (top) and calculated spectra of a single chain (middle) and with the explicit correction for intermolecular interactions (bottom). A basic fragment with 6 monomer units was used in these calculations.

Table 1. Assignments of the peaks of PCL in the THz frequency region (RT: room temperature, a or b: along the *a*, *b* or *c* axis of PCL, w: weak peak).

Experiment	Calculation	Assignment
THz,RT	CAM-B3LYP-GD3BJ /6-31++G**	
47(⊥)	39(⊥,*a*)	C=O(o.p.)+CH_2
	44(⊥,*b*)	C=O(o.p.)+CH_2
	46(⊥,*a*)	C=O(o.p.)+CH_2
67(⊥,//)	64(⊥,*a*,*b*)	COO+CH_2
	68(//,c)^{w}	C=O(i.p.)+CH_2
75(⊥)	70(⊥,*b*)	--
111(⊥)	119(⊥,*a*)	Skeletal deformation
153(⊥)	167(⊥,*b*)	
197(⊥)	187(⊥,*a*)	
216(⊥)	207(⊥,*a*,*b*)	

THz spectroscopy allows us to observe the intermolecular hydrogen bondings of the polymer separately, since hydrogen bondings with different strengths yield different peaks in a THz spectrum. The results of THz and IR spectral analysis, and QCCs all indicate that PCL forms three kinds of weak intermolecular C-H···O=C hydrogen bondings between the CH_2 and C=O groups. This may be one of the causes for the low melting

temperature but high crystallinity of PCL. There are about six interactions in PCL and about sixteen interactions in polyglycolic acid (PGA), within the lamellar thickness. Therefore, it is suggested that the difference in the number of intermolecular interactions within the lamellar thickness leads to the difference in melting points between the two polymers.

The Born-Oppenheimer molecular simulations of infrared spectra of crystalline poly-(R)-3-hydroxybutyrate with analysis of weak C-H···O=C hydrogen bonds

Mateusz. Z. Brela,[1,3] Marek Boczar,[1] Marek J. Wójcik,[1] Harumi Sato, Takahito Nakajima,[2] Yukihiro Ozaki[3]

[1]Jagiellonian University

[2]RIKEN

[3]Kwansei Gakuin University

(*Chem. Phys. Lett*. 2017)

We present results of study of weak C-H···O=C hydrogen bonds of crystalline poly-(R)-3-hydroxybutyrate (PHB) by using Born-Oppenheimer molecular dynamics. The polymeric structure and IR spectra of PHB result from the presence of the weak hydrogen bonds. We applied the post-molecular dynamics analysis to consider a C=O motion as indirectly involved in the hydrogen bonds. Quantization of the nuclear motion of the oxygens was done to perform detailed analysis of the strength and properties of the C=O bands involved in the weak hydrogen bonds. We have also shown the dynamic character of the weak hydrogen bond interactions.

Study of Hydrogen Bond Dynamics in Nylon 6 Crystals Using IR Spectroscopy and Molecular Dynamics Focusing on the Differences Between α and γ Crystal Forms

Mateusz. Z. Brela[1], Marek J. Wójcik[1], Marek Boczar[1], Erika Onishi[2] Harumi Sato, Takahito Nakajima[3], Yukihiro Ozaki[2]

[1]Jagiellonian University

[2]Kwansei Gakuin University

[3]RIKEN

(*Int. J. Quantum Chem. 2018*)

Proton dynamics of hydrogen bonds (HBs) in the α and γ form of Nylon 6 were investigated by Born–Oppenheimer molecular dynamics (BOMD). Our results show differences in the dynamic effects of interchain HB interactions between the α form and the γ form of Nylon 6. Analysis of the time course of the geometrical parameters of HBs along the BOMD simulations has shown that HBs are dynamically favored in the g form of Nylon. The quantization of the NAH stretching mode enables a detailed discussion of the strengths of HB interactions. Solving the Schrödinger equation for the snapshots of one-dimensional proton potentials, extracted from the ab initio MD, enables the consideration of anharmonicity, thermodynamics, and approximate quantum effects on proton movement. A larger red shift of the NAH stretching band was observed in the γ form compared with theαform. Our study shows that HBs are more stabilized in the γ form than in the

α form, which is mainly due to the higher number of HBs. The distribution of HBs along the trajectory clearly reveals the preference of the γ form. The quantization of the NAH motion enables the discussion of the differences in the IR spectra between the two forms.

III Terahertz Material Physics Laboratory

III-A. HIGH FIELD ELECTRON SPIN RESONANCE (ESR) STUDIES OF QUANTUM SPIN SYSTEMS

Quantum spin system shows distinct quantum effects due to its strong quantum fluctuation. Since the proposal of the Haldane's conjecture, which received the Nobel award, quasi-one or two dimensional quantum spin systems have attracted much interest, and their short-range order and their ground state at low temperature should be clarified. High frequency high field ESR turns out to be a powerful means to observe the short-range order and the ground state of the system. Moreover, frustrated magnetic systems have also attracted much interest recently. The frustration in the magnetic system suppresses the conventional magnetic order and a unique ground state appears at low temperature. Especially the competition is expected between the frustration and low dimensionality. Following the trends from a Grant-in-Aid for Scientific Research on Priority Areas "Novel states of matter induced by frustration" (No.473, 2007-2011, Headed by Prof. H. Kawamura (Osaka University) and H. Ohta was a member), we are studying these low dimensional antiferromagnets with frustration and related multiferroic materials intensively. High field ESR measurements of spinel compound $GeCo_2O_4$, which has Co pyrochlore structure of three dimensional frustrated lattice, has been studied. Temperature and wide-range frequency dependence measurements show clearly two successive transitions in the ordered state.

H. Ohta gave an invited presentation at "Dzyaloshinskii-Moriya Interaction and Exotic Spin Structures" (May 23-26, Peterhof, Russia), and S. Okubo organized symposium of S=1/2 diamond chain physics in Japanese Physical Society meeting (Mar 17-20, Osaka, Japan).

In meantime H. Ohta was appointed as the President of International EPR (ESR) Society (IES) since January, 2015 and attended four EPR/ESR related international conferences to increase the visibility of IES by organizing AGM and presenting IES awards. H. Ohta is also acting as the Advisory Council of APES (Asia-Pacific EPR/ESR Society), the President of the Japan Society of Infrared Science and Technology, and the Council Member of SEST.

Moreover, in order to strengthen the pulsed magnetic field researches in western Japan region, we have set up The KOFUC (Kobe-Osaka-Fukui Universities Centers) Network since 2014.

THz ESR study of Spinel Compound $GeCo_2O_4$

Susumu Okubo[1], Hitoshi Ohta[1*], Tatsuya Ijima[2], Tatsuya Yamasaki[2], Wei-Min Zhang[1], Shigeo Hara[3], Shinichi Ikeda[4], Hiroyuki Oshima[5], Miwako Takahashi[5], Keisuke Tomiyasu[6] and Tadatake Watanabe[7]

[1]Molecular Photoscience Research Center, Kobe University

[2]Graduate School for Science, Kobe University

[3]Department of Physics, Chuo University

[4]National Institute of Advance Industrial Science and Technology

[5]Institute of Material Science, University of Tsukuba

[6]Department of Physics, Tohoku University

[7]Department of Physics, College of Science and Technology, Nihon University

(*Z. Phys. Chem.* 2017)

We performed terahertz ESR measurements of spin frustrated spinel compound $GeCo_2O_4$ using pulsed magnetic fields of up to 40 T. A very broad EPR absorption line was observed at 86 K. The g-values at 86 K were estimated to be g=5.26±0.07, 5.16±0.12 and 4.98±0.07 for B//[111], [100] and [110], respectively. High-field ESR measurements revealed complicated phase structures and a field-induced magnetic phase below 3 K. Critical fields of magnetic phases at 1.8 K for B//[111] were observed at 1.8 T, 5.0 T, 8.6 T, 11.0 T and 12.9 T for B//[111]. An energy gap of 300 GHz (=14.4 K=1.24 meV), which was related to the lattice deformation, was observed for B//[111]. The zero field gap of ω4 mode, which is considered to be a singlet-triplet excitation of the di-tetramer, was estimated to be 1120 GHz.

III-B. RESEARCHES ON VVARIOUS PHYSICAL PROPERTIES USING ESR AND MAGNETO-OPTICAL MEASUREMENTS

There are many unsolved basic properties due to technical difficulties, such as the zero-field splitting energy in Fe(III) 3d-electron system. We have investigated such remaining problems using our THz ESR systems. Although study of zero-field splitting energy of Fe(III) ion in bio-related model substance Hemin has been performed for long time, no report on the in-plane anisotropy of Hemin exists. Precise determination of splitting parameters has been made by our high-field and high-frequency ESR system. H. Ohta gave an invited presentation concerning Hemin at EPR2017.

Dirac fermion in topological insulator is one of biggest issue in recent solid state physics. S. Okubo succeeded direct observation of Dirac fermion in surface of topological insulator Bi_2Se_3 using magneto-optical measurements.

Precise Determination of Zero-Field Splitting Parameters of Hemin by High-Field and High-Frequency Electron Paramagnetic

Tsubasa Okamoto[1], Eiji Ohmichi[1], Susumu Okubo[2], and Hitoshi Ohta[2]

[1]Graduate School of Science, Kobe University

[2]Molecular Photoscience Research Center, Kobe University

(*J. Phys. Soc. Jpn.,* 2017)

The zero-field splitting (ZFS) parameters of Fe(III) protoporphyrin IX chloride, or hemin, a model substance of hemoproteins, were determined precisely by high-field and high-frequency electron paramagnetic resonance (HFEPR). From multi-frequency measurements up to 700 GHz, multiple EPR absorptions were clearly resolved, and the rhombic component of ZFS was directly determined, for the first time, as $|E| = 0.055 \pm 0.005$ cm^{-1}, in addition to the axial component $D = 6.90 \pm 0.01$ cm^{-1}. This finding indicates the essential role of the rhombic symmetry of excited states in the ZFS parameters.

III-C. DEVELOPMENT AND APPLICATION OF HIGH-PRESSURE THz ESR SYSTEM

We developed a high-pressure ESR system in THz region with the combination of the hybrid-type piston-cylinder pressure cell having THz window and the cryogen-free 10 T superconducting magnet in 2014 by the collaboration with Prof. Uwatoko (ISSP, University of Tokyo). Recently, the high-pressure ESR measurement has been recognized as a powerful means to study magnetic materials subjected to pressure, especially that in the high field and THz region. We reviewed the reported high-pressure ESR systems with emphasis on the advantages of our system in THz region as the invited paper of J. Mag. Res. The high-pressure THz ESR has also attracted much attention from the viewpoint of the application of the crystal field theory. We collaborated with Prof. Rudowicz (Mickiewicz University, Poland), who is an expert in crystal field theory, to investigate an analysis method for ESR data of high-spin species and their pressure effect. The high-pressure THz ESR system was applied to the Shastry-Sutherland Model compound $SrCu_2(BO_3)_2$, and the pressure induced phase transition was discovered at 1.85 GPa for the first time. The analyses gave good agreements with the predicted theories.

H. Ohta gave an invited presentation about the pressure induced phase transition on $SrCu_2(BO_3)_2$ at LT2017. H. Ohta also gave invited presentations at AWEST and MDMR2017, and at two seminars concerning the developments of high pressure THz ESR.

High-field/high-pressure ESR

T. Sakurai[1], S. Okubo[2] and H. Ohta[2]

[1]Research Facility Center for Science and Technology, Kobe University

[2]Molecular Photoscience Research Center, Kobe University

(*J. Mag. Res.,* 2017)

We present a historical review of high-pressure ESR systems with emphasis on our recent development of a high-pressure, high-field, multi-frequency ESR system. Until 2000, the X-band system was almost established using a resonator filled with dielectric materials or a combination of the anvil cell and dielectric resonators. Recent developments have shifted from that in the low-frequency region, such as X-band, to that in multi-frequency region. High-pressure, high-field, multi-frequency ESR systems are classified into two types. First are the systems that use a vector network analyzer or a quasi-optical bridge, which have high sensitivity but a limited frequency region; the second are like our system, which has a very broad frequency region covering the THz region, but lower sensitivity. We will demonstrate the usefulness of our high-pressure ESR system, in addition to its experimental limitations. We also discuss the recent progress of our system and future plans.

High-frequency EMR data for Fe^{2}+ (S=2) ions in natural and synthetic forsterite revisited - Fictitious spin S'=1 versus effective spin S=2 approach

M. Kozanecki[1], C. Rudowicz[1], H. Ohta[2] and T. Sakurai[3]

[1]Faculty of Chemistry, A. Mickiewicz University
[2]Molecular Photoscience Research Center, Kobe University
[3]Center for Supports to Research and Education Activities, Kobe University
(*Journal of Alloys and Compounds,* 2017)

Recent wide-band (65 ‑ 850 GHz) electron magnetic resonance (EMR) study determined the zero field splitting (ZFS) parameters (ZFSPs) for Fe^{2+} in natural and synthetic forsterite (Mg_2SiO_4) based on the fictitious spin S' = 1 approach. So-obtained ZFSPs (D', E') are incompatible with those available in literature for $3d^6$ (Fe^{2+}) and $3d^4$ (Fe^{4+}, Mn^{3+}, Cr^{2+}) ions with the electronic spin S = 2, which predominantly pertain to the effective spin S = 2. Background for the effective spin S versus the fictitious ' spin ' S' (J') approaches is provided with focus on application to Fe^{2+} ions. To enable comparison of the S' = 1 ZFSPs with the S = 2 ones methodology for conversions has been worked out and appropriate conversion relations derived for various combinations of the possible energy level schemes for the spin S = 2 and S'= 1. The second-rank S'= 1 ZFSPs (D', E') measured by high-frequency EMR for Fe^{2+} in Mg_2SiO_4 are converted to the S = 2 ZFSPs (D, E) and compared with literature data. Suitability of Fe^{2+}:Mg_2SiO_4 systems for application as high-pressure probes for high-magnetic field and high-frequency EMR (HMF-EMR) is then considered. The results of this study may be applied to other cases of $3d^6$ and $3d^4$ (S = 2) ions in various hosts.

Spectroscopic and magnetic properties of Fe^{2+} ($3d^6$; S = 2) ions in Fe $(NH_4)_2(SO_4)_26H_2O$ – Modeling zero-field splitting and Zeeman electronic parameters by microscopic spin Hamiltonian approach

M. Zajac[1], C. Rudowicz[2], H. Ohta[3] and T. Sakurai[4]

[1]Institute of Physics, West Pomeranian University of Technology
[2]Faculty of Chemistry, A. Mickiewicz University
[3]Molecular Photoscience Research Center, Kobe University
[4]Center for Supports to Research and Education Activities, Kobe University
(*J. Magn. Magn. Mat.,* 2018)

Utilizing the package MSH/VBA, based on the microscopic spin Hamiltonian (MSH) approach, spectroscopic and magnetic properties of Fe^{2+} ($3d^6$; S = 2) ions at (nearly) orthorhombic sites in $Fe(NH_4)_2(SO_4)_2{\cdot}6H_2O$ (FASH) are modeled. The zero-field splitting (ZFS) parameters and the Zeeman electronic (Ze) factors are predicted for wide ranges of values of the microscopic parameters, i.e. the spin-orbit (λ), spin-spin (ρ) coupling constants, and the crystal-field (ligand-field) energy levels (Δi) within the ^5D multiplet. This enables to consider the dependence of the ZFS parameters (in the Stevens notation), or the conventional ones (e.g., D and E), and the Zeeman factors gi on λ, ρ, and Δi. By matching the theoretical SH parameters and the experimental ones measured by electron magnetic resonance (EMR), the values of λ, ρ, and Δi best describing Fe^{2+} ions in FASH are determined. The novel aspect is prediction of the fourth-rank ZFS parameters and the

ρ(spin-spin)-related contributions, not considered in previous studies. The higher-order contributions to the second- and fourth-rank ZFSPs are found significant. The MSH predictions provide guidance for high-magnetic field and high-frequency EMR (HMF-EMR) measurements and enable assessment of suitability of FASH for application as high-pressure probes for HMF-EMR studies. The method employed here and the present results may be also useful for other structurally related Fe^{2+} ($S = 2$) systems.

Electron magnetic resonance data on high-spin Mn(III; S= 2) ions in porphyrinic and salen complexes modeled by microscopic spin Hamiltonian approach

Krzysztof Tadyszak[1,2], Czesław Rudowicz[3,4], Hitoshi Ohta[5,6], Takahiro Sakurai[7]

[1]NanoBioMedical Centre, Adam Mickiewicz University, Poland

[2]Institute of Molecular Physics, Polish Academy of Sciences, Poland

[3]Visiting Professor: Faculty of Chemistry, A. Mickiewicz University, Poland

[4]On leave of absence from: Modeling in Spectroscopy Group, Institute of Physics, West Pomeranian University of Technology Szczecin, Poland

[5]Graduate School of Science, Kobe University

[6]Molecular Photoscience Research Center, Kobe University

[7]Center for Supports to Research and Education Activities, Kobe University

(*J. Inorg. Biochem.* 2017)

The spin Hamiltonian (SH) parameters experimentally determined by EMR (EPR) may be corroborated or otherwise using various theoretical modeling approaches. To this end semiempirical modeling is carried out for high-spin (S = 2) manganese (III) 3d4 ions in complex of tetraphenylporphyrinato manganese (III) chloride (MnTPPCl). This modeling utilizes the microscopic spin Hamiltonians (MSH) approach developed for the 3d4 and 3d6 ions with spin S=2 at orthorhombic and tetragonal symmetry sites in crystals, which exhibit an orbital singlet ground state. Calculations of the zero-field splitting (ZFS) parameters and the Zeeman electronic (Ze) factors (g||=gz, g⊥=gx =gy) are carried out for wide ranges of values of the microscopic parameters using the MSH/VBA package. This enables to examine the dependence of the theoretically determined ZFS parameters bkq (in the Stevens notation) and the Zeeman factors gi on the spin-orbit (λ), spin-spin (ρ) coupling constant, and the ligand-field energy levels (Δi) within the ^5D multiplet. The results are presented in suitable tables and graphs. The values of λ, ρ, and Δi best describing Mn(III) ions in MnTPPCl are determined by matching the theoretical second-rank ZFSP $b_20(D)$ parameter and the experimental one. The fourth-rank ZFS parameters (b_40, b_4^4) and the ρ (spin-spin)-related contributions, which have been omitted in previous studies, are considered for the first time here and are found important. Semiempirical modeling results are compared with those obtained recently by the density functional theory (DFT) and/or ab initio methods.

Direct Observation of the Quantum Phase Transition of $SrCu_2(BO_3)_2$ by High-Pressure and Terahertz Electron Spin

T. Sakurai[1], Y. Hirao[2], K. Hijii[3], S. Okubo[3], Hitoshi Ohta[3], Y. Uwatoko[4], K. Kudo[5], and Y. Koike[6]

[1]Research Facility Center for Science and Technology, Kobe University

[2]Graduate School of Science, Kobe University

[3]Molecular Photoscience Research Center, Kobe University

[4]Institute for Solid State Physics, University of Tokyo

[5]Research Institute for Interdisciplinary Science, Okayama University

[6]Department of Applied Physics, Tohoku University

(*J.Phys. Soc. Jpn.,* 2018)

High-pressure and high-field electron spin resonance (ESR) measurements have been performed on a single crystal of the orthogonal-dimer spin system $SrCu_2(BO_3)_2$. With frequencies below 1 THz, ESR signals associated with transitions from the singlet ground state to the one-triplet excited states and the two-triplet bound state were observed at pressures up to 2.1 GPa. We obtained directly the pressure dependence of the gap energies, finding a clear first-order phase transition at Pc = 1.85 ± 0.05 GPa. By comparing this pressure dependence with the calculated excitation energies obtained from an exact diagonalization, we determined the precise pressure dependence for inter- (J') and intra-dimer (J) exchange interactions considering the Dzyaloshinski‐Moriya interaction. Thus this system undergoes a first-order quantum phase transition from the dimer singlet phase to a plaquette singlet phase above the ratio (J'/J)c = 0.660 ± 0.003.

III-D. DEVELOPMENT OF BROADBAND FORCE-DETECTED ESR TECHNIQUES USING MICRO-CANTILEVER AND NANOMEMBRANE

High-frequency and high-field ESR measurement has many advantages compared with the conventional X-band ESR such as high spectral resolution, and ESR detection of spin systems possessing a large zero-field splitting. However, ESR measurements using the millimeter and terahertz (THz) waves have the sensitivity limitation at the moment. Therefore, a new, highly sensitive detection technique for THz ESR compatible with a high magnetic field is required for its wide application, and we are developing the highly sensitive force-deteced ESR system using micromechanical devices. E. Ohmichi is working on the microfabrication of MEMS cantilever for mechanically detected ESR. E. Ohmichi and H. Takahashi developed a high-sensitivity force/torque-detected ESR system based on a commercial nanomembrane. The paper by H. Takahashi was selected as "Papers of Editors' choice" from JPSJ. The doctor course student T. Okamoto received the Springer Best Poster Award at AWEST2017, and the Best Presentation Award at the SEST2017 annual meeting.

E. Ohmichi gave invited presentations on his broadband ultrasensitive ESR system at THz-Bio2017 (Italy, 5 Oct 2017) and Toyota Riken Symposium “Dynamic Optical Control of Spin Orders” (Nagoya, 19 Oct 2017). H. Takahashi gave an invited talk on his nanomembrane magnetometer at MANA International Symposium (6 Mar 2018)

H. Ohta gave an invited presentation about the highly sensitive force-detected ESR system at 3 international conferences including MDMR2017 and at two seminars.

Force-detected ESR Measurements in a Terahertz Range up to 0.5 THz and Application to Hemin

T. Okamoto[1], H. Takahashi[2], E. Ohmichi[1], and H. Ohta[3]

[1]Graduate School of Science Kobe University

[2]Organization for Advanced and Integrated Research Kobe University

[3]Molecular Photoscience Research Center, Kobe University

(*Appl. Magn. Reson.,* 2017)

We report a novel force-detected high-frequency electron spin resonance (HFESR) technique using a microcantilever in the terahertz region. In this technique, we attach a tiny sample on the microcantilever end and the ESR signal is detected as the cantilever bending. The bending is sensitively detected by fiber-optic Fabry–Perot interferometry. We applied this technique to a tiny amount (~16 ng) of metalloporphyrin, a model substance of hemoproteins, and successfully observed ESR signals at multiple frequencies up to 0.5 THz. This result indicates that the sample volume needed in multi-frequency HFESR can be greatly reduced by several orders of magnitude, and our novel technique would be a promising tool for HFESR studies of metalloproteins in the future.

New Method for Torque Magnetometry Using a Commercially Available Membrane-Type Surface Stress Sensor

H. Takahashi[1], K. Ishimura[2], T. Okamoto[2], E. Ohmichi[2], and H. Ohta[3]

[1]Organization for Advanced and Integrated Research, Kobe University

[2]Graduate School of Science, Kobe University

[3]Molecular Photoscience Research Center, Kobe University

(*J. Phys. Soc. Jpn.,* 2017)

We present a new method for torque magnetometry by using a commercially available membrane-type surface stress sensor (MSS). This sensor has a silicon membrane supported by four beams in which piezoresistive paths are integrated. Although originally developed as a gas sensor, it can be used for torque measurement by modifying its on-chip aluminum interconnections. We demonstrate the magnetic-torque measurement of submillimeter-sized crystals at low temperature and in strong magnetic fields. This MSS can observe de-Haas–van-Alphen oscillation, which confirms that it can be an alternative tool for self-sensitive microcantilevers.

Mechanically detected terahertz electron spin resonance using SOI-based thin piezoresistive microcantilevers

E. Ohmichi[1], T. Miki[2], H. Horie[2], T. Okamoto[2], H. Takahashi[3], Y. Higashi[4], S. Itoh[4] and H. Ohta[5]

[1]Graduate School of Science, Kobe University

[2] Graduate School of Science, Kobe University

[3]Organization for Advanced and Integrated Research, Kobe University

[4]Graduate School of Science, Kyoto University

[5]Molecular Photoscience Research Center, Kobe University

(*J. Mag. Res*., 2017)

We developed piezoresistive microcantilevers for mechanically detected electron spin resonance (ESR) in the millimeter-wave region. In this article, fabrication process and device characterization of our self-sensing microcantilevers are presented. High-frequency ESR measurements of a microcrystal of paramagnetic sample is also demonstrated at multiple frequencies up to 160 GHz at liquid helium temperature. Our fabrication is based on relatively simplified processes with silicon-on-insulator (SOI) wafers and spin-on diffusion doping, thus enabling cost-effective and time-saving cantilever fabrication.

Force- and torque-detection of high-frequency electron spin resonance using a membrane-type surface-stress sensor

Takahashi H[1], Ishimura K[2], Okamoto T[2], Ohmichi E[2], and Ohta H[3]

[1]Organization for Advanced and Integrated Research, Kobe University

[2]Graduate School of Science, Kobe University

[3]Molecular Photoscience Research Center, Kobe University

(*Rev. Sci. Intrum.* 2018)

We developed a practical useful method for force- and torque-detected electron spin resonance (FDESR/TDESR) spectroscopy in the millimeter wave frequency region. This method uses a commercially available membrane-type surface-stress (MSS) sensor. The MSS is composed of a silicon membrane supported by four beams in which piezoresistive paths are integrated for detecting the deformation of the membrane. Although this device has a lower spin sensitivity than a microcantilever, it offers several distinct advantages, including mechanical strength, ease of use, and versatility. These advantages make this device suitable for practical applications that require FDESR/TDESR.

III-E. MAGNETIZATION MEASUREMENTS USING SQUID MAGNETOMETER

The installation of SQUID magnetometer in 2010 by a Grant-in-Aid Creative Scientific Research "Development of properties and functionalities by precise control of rare-earth doping" (2007-2011, Prof. Y. Fujiwara (Osaka University)) opened up wide varieties of collaborative researches. From 2010 applied materials of SQUID magnetometer spread out continuously. Users of SQUID magnetometer are Mochida

and Takahashi groups, Uchino group (Department of Chemistry, Kobe University), Sugawara and Matsuoka group (Department of Physics, Kobe University), T. Sakurai and S. Hara (Center for Supports to Research and Education Activities, Kobe University). It is also used for the development of SQUID ESR. T. Okamoto, T. Sakurai, E. Ohmichi and H. Ohta received the Excellent Paper Award from the Japan Society of Infrared Science and Technology by the paper concerning the SQUID ESR of hemoproteins.

Thermochromic Magnetic Ionic Liquids from Cationic Nickel(II) Complexes Exhibiting Intramolecular Coordination Equilibrium

Xue Lan[1], Tomoyuki Mochida[1], Yusuke Funasako[2], Kazuyuki Takahashi[1], Takahiro Sakurai[3], and Hitoshi Ohta[4,5]

[1]Department of Chemistry, Graduate School of Science, Kobe University

[2]Department of Applied Chemistry, Faculty of Engineering, Tokyo University of Science

[3]Center for Supports to Research and Education Activities, Kobe University

[4]Department of Physics, Graduate School of Science, Kobe University

[5]Molecular Photoscience Research Center, Kobe University

(*Chem. Eur. J.,* 2016)

Among the various thermochromic materials, liquid thermochromic materials are comparatively rare. To produce functional thermochromic liquids, we have designed ionic liquids based on cationic nickel complexes with either side chains, [Ni(acac)(Me_2 NC_2 H_4 NR^1 R^2)]Tf_2 N ([1]Tf_2 N: R^1 =C_3 H_6 OEt, R^2 =Me; [2]Tf_2 N: R^1 =C_3 H_6 OMe, R^2 =Me; [3]Tf_2 N: R^1 =R^2 =C_3 H_6 OMe), where acac=acetylacetonate and Tf_2 N=(F_3 CSO_2)$_2$ N- . The side chains (R^1, R^2) can moderately coordinate to the metal center, enabling temperature-dependent coordination equilibria in the liquid state. [1]Tf_2 N is a liquid at room temperature. [2]Tf_2 N is obtained as a solid (T_m =352.7 K) but remains liquid at room temperature after melting. [3]Tf_2 N is a solid with a high melting point (T_m = 422.3 K). These salts display thermochromism in the liquid state, appearing red at high temperatures and orange, light-blue, or bluish-green at lower temperatures, and exhibiting concomitant changes in their magnetic properties. This phenomenon is based on temperature-dependent equilibrium between a square-planar diamagnetic species and a paramagnetic species with intramolecular ether coordination.

Single-crystal-to-single-crystal transformation in hydrogen-bond- induced high-spin pseudopolymorphs from protonated cation salts with a π-extended spin crossover Fe(III) complex anion

S. Murata[1], K. Takahashi[1], T. Sakurai[2], H. Ohta[3]

[1]Department of Chemistry, Kobe University

[2]Research Facility Center for Science and Technology, Kobe University

[3]Molecular Photoscience Research Center, Kobe University

(*Polyhedron*, 2017)

Novel pseudopolymorphic Hdabco compounds with an Fe(III) complex anion, (Hdabco)[Fe(aznp)$_2$] · CH_2Cl_2 1 and (Hdabco)[Fe(aznp)$_2$] · 0.5H_2O 2 [dabco = 1,4-diazabicyclo[2.2.2]octane, H_2aznp = (2'-hydroxyphenylazo)-2-hydroxynaphthalene], were prepared and characterized. The magnetic susceptibility for 1 and 2 revealed that both complexes were in a high-spin (HS) state in the whole temperature range and exhibited weak ferromagnetic interactions below 40 K. The crystal structural analyses suggested that strong N–H···O hydrogen bonding interactions between the Hdabco cation and [Fe(aznp)$_2$] anion may induce the distortion of a coordination structure resulting in the HS complexes, whereas π-stacking interactions between the π-ligands in the [Fe(aznp)$_2$] anion and additional C‒H···N hydrogen bonding interactions between the Hdabco cation and [Fe(aznp)$_2$] anion constructed a intermolecular interaction framework structure with one-dimensional channels. The thermosgravimetry analysis for compound 1 indicated the adsorption of a water molecule took place after the desorption of a dichloromethane molecule. This transformation of 1 into 2 proved to proceed in a single-crystal-to-single-crystal way by powder X-ray diffractions and single crystal X-ray structural analysis.

Valence control of ionic molecular crystals: effect of substituents on the structures and valence states of biferrocenium salts

T. Mochida[1], Y. Funasako[2], H. Kimata[1], T. Tominaga[1], T. Sakurai[3], H. Ohta[4]

[1]Department of Chemistry, Graduate School of Science, Kobe University

[2]Department of Applied Chemistry, Faculty of Engineering, Tokyo University of Science

[3]Research Facility Center for Science and Technology, Kobe University

[4]Department of Physics, Graduate School of Science, Kobe University

(*Crystal Growth & Design,* 2017)

In this work, the effect of substituents on the valence states of biferrocenium salts was investigated in order to explore the valence control of ionic molecular materials. Reactions of 1',1‴-disubstituted biferrocene derivatives (R_2-bifc) and fluoro tetracyanoquinodimethanes (F_n-TCNQ; n = 1, 2, 4) produced single crystals of six salts (1–6), most of which were either monovalent ($[D]^+[A_m]^-$; m = 1–3) or divalent ($[D]^+[A_m]^-$) salts. (Et_2-bifc)(F_1-TCNQ)$_2$ (1) was a mixed-stack monovalent salt, whereas the corresponding F_2-TCNQ salt was a divalent salt. (MeO_2-bifc)(F_1-TCNQ)$_2$ (2) was a monovalent salt because of the small Madelung energy of its segregated-stack structure, despite the low redox potential of the donor. (MeS_2-bifc)(2,6-F_2-TCNQ)$_2$ (3) was a mixed-stack salt with an apparent intermediate valence state ($[D]^{1.5+}[A_2]^{1.5-}$), containing $[D]^{2+}$ and $[D]^+$ in a 1:1 ratio. Its valence state, which is intermediate between those of corresponding salts with F_1-TCNQ and 2,5-F_2-TCNQ, is probably related to the unsymmetrical crystalline environment. (Bu_2-bifc)(F_1-TCNQ)$_3$ (4) was a divalent salt with a segregated-stack structure, whereas the corresponding TCNQ salt was

monovalent. (R_2-bifc)(F_4-TCNQ) [R = Bu (5), I (6)] were monovalent salts. Their magnetic susceptibilities were found to be consistent with their valence states. These results demonstrated that the valence control of biferrocenium salts could be achieved via the fluorine substitution of acceptors and crystal engineering.

Possible Frustration Effects on a New Antiferromagnetic Compound $Ce_6Pd_{13}Zn_4$ with the Octahedral Ce Sublattices

E. Matsuoka[1], A. Oshima[1], H. Sugawara[1], T. Sakurai[2], H. Ohta[3]

[1]Department of Physics, Graduate School of Science, Kobe University

[2]Research Facility Center for Science and Technology, Kobe University

[3]Molecular Photoscience Research Center, Kobe University

(*J. Phys. Soc. Jpn*., 2017)

Magnetization, specific heat, and electrical resistivity measurements have been performed on polycrystalline samples of a new cubic compound, $Ce_6Pd_{13}Zn_4$. This compound exhibits metallic behavior and is classified as a Kondo-lattice system. The trivalent Ce ions are responsible for the antiferromagnetic transition at T_N = 3.3 K and the phase transition at T'_N=1.3K with the formation of superzone gaps. The increase in magnetic susceptibilities below TN and the considerably large value of the specific heat divided by temperature (1.25 J·Ce-mol^{-1}·K^{-2}) imply the existence of non-ordered Ce magnetic moments due to the geometrical frustration on the octahedral Ce sublattice.

Paramagnetic ionic plastic crystals containing the octamethylferrocenium cation: counteranion dependence of phase

T. Mochida[1], M. Ishida[1], T. Tominaga[1], K. Takahashi[1], T. Sakurai[2], H. Ohta[3,4]

[1]Department of Chemistry, Graduate School of Science, Kobe University

[2]Research Facility Center for Science and Technology, Kobe University,

[3]Department of Physics, Graduate School of Science, Kobe University

[4]Molecular Photoscience Research Center, Kobe University

(*Phys. Chem. Chem Phys.,* 2017)

In recent years, ionic plastic crystals have attracted much attention. Many metallocenium salts exhibit plastic phases, but factors affecting their phase transitions are yet to be elucidated. To investigate these factors, we synthesized octamethylferrocenium salts with various counteranions [Fe($C_5Me_4H)_2$]X ([1]X; X$^-$ = $B(CN)_4^-$, $C(CN)_3^-$, $N(CN)_2^-$, FSA (= $(SO_2F)_2N^-$), $FeCl_4^-$, $GaCl_4^-$ and CPFSA (= $CF_2(SO_2CF_2)_2N^-$)) and elucidated their crystal structures and phase behavior. Correlations between the crystal structures and phase sequences, and the shapes and volumes of the anions are discussed. Except for [1][CPFSA], these salts exhibit phase transitions to plastic

phases at or above room temperature (T_C = 298–386 K), and the plastic phases exhibit either NaCl- or anti-NiAs-type structures. X-ray crystal structure analyses of these salts at 100 K revealed that they have structures in which cations and anions are alternately arranged, with the exception of [1][CPFSA]. [1][CPFSA] exhibits a structure in which anions and cations are separately stacked to form columns. [1][$N(CN)_2$] exhibits a polar crystal structure that undergoes a monotropic phase transition to a centrosymmetric structure. The magnetic susceptibilities of room-temperature plastic crystals [1][$GaCl_4$] and [1][$FeCl_4$] were investigated; the latter exhibits a small ferromagnetic interaction at low temperatures.

Contribution of Coulomb Interactions to a Two-Step Crystal Structure Phase Transformation Coupled with a Significant Change in Spin Crossover Behavior for a Series of Charged Fe^{II} Complexes from 2,6-Bis (2-methylthiazol-4-yl) pyridine

K. Takahashi[1], M. Okai[1], T. Mochida[1], T. Sakurai[2], H. Ohta[3], T. Yamamoto[4], Y. Einaga[4], Y. Shiota[5], K. Yoshizawa[5], H. Konaka[6], A. Sasaki[6]

[1]Department of Chemistry, Graduate School of Science, Kobe University

[2]Research Facility Center for Science and Technology, Kobe University

[3]Molecular Photoscience Research Center, Kobe University

[4]Department of Chemistry, Faculty of Science and Technology, Keio University

[5]Institute for Materials Chemistry and Engineering, Kyushu University

[6]XRD Application & Software Development, Rigaku Corporation

(*Inorg. Chem.*, 2018)

A series of $[Fe^{II}(L)_2](BF_4)_2$ compounds were structurally and physically characterized (L = 2,6-bis(2-methylthiazol-4-yl)pyridine). A crystal structure phase transformation from dihydrate compound 1 to anhydrous compound 3 through partially hydrated compounds 2 and 2’ upon dehydration was found. Compounds 1 and 3 exhibited a gradual spin crossover (SCO) conversion, whereas compounds 2 and 2’ demonstrated two-step and one-step abrupt SCO transitions, respectively. An X-ray single-crystal structural analysis revealed that one-dimensional and two-dimensional Fe cation networks linked by π stacking and sulfur‑sulfur interactions were formed in 1 and 3, respectively. A thermodynamic analysis of the magnetic susceptibility for 1, 2’, and 3 suggests that the enthalpy differences may govern SCO transition behaviors in the polymorphic compounds 2’ and 3. A structural comparison between 1 and 3 indicates that the SCO behavior variations and crystal structure transformation in the present $[Fe^{II}(L)_2](BF_4)_2$ compounds can be interpreted by the relationship between the lattice enthalpies mainly arising from Coulomb interactions between the Fe cations and BF_4 anions as in typical ionic crystal.

Application of a high-frequency ESR technique using a SQUID magnetometer to a model complex of hemoproteins (in Japanese)

T. Okamoto[1], T. Sakurai[2], E. Ohmichi[1], H. Ohta[3]

[1]Graduate School of Science, Kobe University

[2]Research Facility Center for Science and Technology, Kobe University

[3]Molecular Photoscience Research Center, Kobe University

(*J. Jpn. Soc. Infrared Science & Technology,* 2017)

Electron spin resonance (ESR) in a terahertz (THz) range is a powerful method for studying microscopic properties of samples. We have applied our magnetically detected high-frequency ESR technique to hemin which is one of the model complexes of hemoprotein. In this study, we used a commercial SQUID (Superconducting QUantum Interference Device) magnetometer as a sensitive detector of sample magnetization and combined it with high-frequency light sources. We have successfully observed ESR signals of polycrystalline hemin sample in frequencies up to 160 GHz as a change of the sample magnetization and determined g-value and axial zero-field splitting parameter *D*. We have also analyzed ESR-induced magnetization changes quantitatively, taking an advantage of a commercial SQUID magnetometer. Our high-frequency ESR technique using a SQUID magnetometer will be useful in studying hemoproteins such as hemoglobin or myoglobin to elucidate the local electronic structure and functional roles in biological systems.

III-E. SPIN AND LATTICE DYNAMICS STUDIED BY PUMP-PROBE AND TERAHERTZ SPECTROSCOPIES

The terahertz region in the electromagnetic spectrum has attracted research attention in solid-state physics, because elementary excitations in solid-state materials such as phonons and magnons play important roles, and many of those dynamics appear in this energy region. The ultrafast spin dynamics and optical spin control in magnetic materials are attractive topics because of the potential applications in the developments of ultrafast spin control, spintronics, quantum computing, and optical control of correlated spin systems. We studied the spin and lattice dynamics in solid-state materials using optical pump-probe spectroscopy and terahertz time-domain spectroscopy (THz-TDS). The generation and detection of magnetization and birefringence using optical and electric pulses are very useful to observe the spin and lattice dynamics in ferromagnetic, antiferromagnetic, multiferroic, and magnetoelectric materials. The time-domain spectroscopy has a large potential for the ultrafast, broadband, and accurate observation of elementary excitation dynamics in the terahertz region.

Observation of Ultrafast Magnon Dynamics in Antiferromagnetic Nickel Oxide by Optical Pump-Probe and Terahertz Time-Domain Spectroscopies

Toshiro Kohmoto[1,2], Takeshi Moriyasu[3], Suguru Wakabayashi[1], Hogyun Jinn[1], Masayuki

Takahara[1], and Kenji Kakita[1]

[1]Graduate School of Science, Kobe University

[2]Molecular Photoscience Research Center, Kobe University

[3]University of Fukui

(*J. Infrared Milli. Terahz. Waves, 2017*)

We have studied the ultrafast magnon dynamics in an antiferromagnetic 3d-transition-metal monoxide, nickel oxide (NiO), using optical pump-probe spectroscopy and terahertz time-domain spectroscopy (THz-TDS). THz damped magnon oscillations were observed in the Faraday rotation signal and in the transmitted THz electric field via optical pump-probe spectroscopy and THz-TDS, respectively. The magnon signals were observed in both the optical pump-probe spectroscopy and THz-TDS experiments, which shows that both Raman- and infrared-active modes are included in the NiO magnon modes. The magnon relaxation rate observed using THz-TDS was found to be almost constant up to the Néel temperature T_N (= 523 K), and to increase abruptly near that temperature. This shows that temperature-independent spin-spin relaxation dominates up to T_N. In our experiment, softening of the magnon frequency near T_N was clearly observed. This result shows that the optical pump-probe spectroscopy and THz-TDS have high frequency resolution and a high signal to noise ratio in the THz region. We discuss the observed temperature dependence of the magnon frequencies using three different molecular field theories. The experimental results suggest that the biquadratic contribution of the exchange interaction plays an important role in the temperature dependence of the sublattice magnetization and the magnon frequency in cubic antiferromagnetic oxides.

Dynamics of the Electric-Field Induced Magnetization in YIG Observed by Faraday Rotation

Takashi Hasunuma[1] and Toshiro Kohmoto[1,2]

[1]Graduate School of Science, Kobe University

[2]Molecular Photoscience Research Center, Kobe University

(*SpinTECH 2017*)

Yttrium iron garnet (YIG, $Y_3Fe_5O_{12}$) is a ferrimagnetic material with a Curie temperature 560 K and is known to show a large Faraday effect. It has been reported that YIG shows a second-order magnetoelectric effect at room temperature and a first-order magnetoelectric effect below 125 K. Furthermore, a second-order magnetoelectric effect at low temperatures was reported in the recent study. In the present study, we observed the electric-field induced magnetization caused by the magnetoelectric effect in YIG (0.3 mm) at room temperature. The nanosecond dynamics of the magnetization after an electric-field pulse are detected as the Faraday rotation of a transmitted probe pulse (800 nm). In our experiment, the electric and magnetic fields were applied parallel to the direction of the probe beam. The Faraday rotation signal observed at room temperature in a magnetic field and a stepped electric field shows damped oscillations in the nanosecond region. The observed Faraday rotation amplitude has linear dependence on the electric field, which suggests the first-order magnetoelectric effect. The Faraday rotation signal disappears in the magnetic field above 0.16 T. It is considered that the

disappearance of the Faraday rotation signal is caused by the saturation of the magnetization.

Magnetic-Field Dependence of the Coherent Magnons in an Antiferromagnet NiO

Kensho Kawamoto[1], Masahiro Tatematsu[1], and Toshiro Kohmoto[1,2]

[1]Graduate School of Science, Kobe University

[2]Molecular Photoscience Research Center, Kobe University

(*SpinTECH 2017*)

In recent years, ultrafast spin control has attracted much attention, and the spin dynamics of antiferromagnets has been investigated widely. Previously, we observed the terahertz oscillations of coherent magnons using polarization spectroscopy with the pump-probe technique in a biaxial antiferromagnet nickel oxide (NiO), whose Néel temperature T_N is 523 K. The magnon modes of 1.0 THz are found to be degenerate near room temperature.

In this study, we observed the coherent magnons in NiO in the magnetic field up to 5 T at room temperature using the transmission pump-probe technique. In the experiment, a sample crystal (0.1-mm thickness) is excited with a circularly polarized pump pulse (800 nm, 0.2 ps) to generate coherent magnons, and their oscillations are detected as the Faraday rotation of a probe pulse (900 nm, 0.2 ps).

Magnon oscillations were observed in the applied magnetic field up to 5 T, and the magnon spectrum was obtained from the Fourier transform of the oscillation signal. In this experiment, degeneracy lifting of magnon modes was not observed. The magnon frequency shifts to the higher frequency side as the magnetic field increases. The behavior of the observed magnon frequency can be explained by the magnetic-field dependence of the antiferromagnetic resonance frequency in a simple theory for biaxial antiferromagnets.

Original Papers 発表論文

authors	title	journal	Vol.	page	year
K. Tada, M. Hirata, and S. Kasahara	Hyperfine interaction constants of $^{14}NO_2$ in 14500－16800 cm^{-1} energy region	*J. Chem. Phys.*	**147**	164304	2017.10.24
Daphné V. Lubert-Perquel, Enrico Salvadori, Matthew Dyson1, Paul N. Stavrinou, Riccardo Montis, Hiroki Nagashima, Yasuhiro Kobori, Sandrine Heutz1 and Christopher W. M. Kay	Formation of Distinct Quintet States in Ordered Organic Semiconductor Films	*arXiv*	-	arXiv:1801.00603v2	2018.1.3
Yuta Yamamoto, Takumi Ako, Takashi Tachikawa, Itaru Osaka, Yasuhiro Kobori	Time-Resolved EPR Study on Photoinduced Charge-Transfer Trap State in Thiophene-Thiazolothiazole Copolymer Film	*J. Photopolym. Sci. Technol.*	**30**	551-555	2017.6.29
Peng Zhang, Tomoya Ochi, Mamoru Fujitsuka, Yasuhiro Kobori, Tetsuro Majima, Takashi Tachikawa	Topotactic Epitaxy of $SrTiO_3$ Mesocrystal Superstructures with Anisotropic Construction for Efficient Overall Water Splitting	*Angew. Chem. Int. Ed.*	**56**	5299-5303	2017.4.6
Izuru Karimata, Yasihiro Kobori, Takashi Tachikawa	Direct Observation of Charge Collection at Nanometer-Scale Iodide-Rich Perovskites during Halide Exchange Reaction on $CH_3NH_3PbBr_3$	*J. Phys. Chem. Lett.*	**8**	1724–1728	2017.4.20
Peng Zhang, Takashi Tachikawa, Mamoru Fujitsuka, and Tetsuro Majima	The Development of Functional Mesocrystals for Energy Harvesting, Storage, and Conversion	*Chem. -Eur. J.*	**24**	in press	2017.12.13
Jessica Afalla, Kaoru Ohta, Shunrou Tokonami, Elizabeth Ann Prieto, Gerald Angelo Catindig, Karl Cedric Gonzales, Rafael Jaculbia, John Daniel Vasquez, Armando Somintac, Arnel Salvador, Elmer Estacio, Masahiko Tani, and Keisuke Tominaga	Charge carrier dynamics of GaAs/AlGaAs asymmetric double quantum wells at room temperature studied by optical pump terahertz probe spectroscopy	*Japanese Journal of Applied Physics*	**56** (11)	111203	2017.10.25
Kaoru Ohta, Shunrou Tokonami, Kotaro Takahashi, Yuto Tamura, Hiroko Yamada, and Keisuke Tominaga	Probing Charge Carrier Dynamics in Porphyrin-Based Organic Semiconductor Thin Films by Time-Resolved THz Spectroscopy	*J. Phys. Chem. B*	**121** (43)	10157–10165	2017.10.12
Masaki Okuda, Kaoru Ohta, and Keisuke Tominaga	Rotational Dynamics of Solutes with Multiple Single Bond Axes Studied by Infrared Pump-Probe Spectroscopy	*J. Phys. Chem. A*	**122** (4)	946–954	2017.12.27
Naoki Yamamoto, Shota Ito, Masahiro Nakanishi, Eri Chatani, Keiichi Inoue, Hideki Kandori, Keisuke Tominaga	Effect of Temperature and Hydration Level on Purple Membrane Dynamics Studied Using Broadband Dielectric Spectroscopy from Sub-GHz to THz Regions	*J. Phys. Chem. B*	**122** (4)	1367–1377	2018.1.5
Masaki Okuda, Masahiro Higashi, Kaoru Ohta, Shinji Saito, and Keisuke Tominaga	Theoretical investigation on vibrational frequency fluctuations of SCN-derivatized vibrational probe molecule in water	*Chemical Physics*		In press	2018.3.12

Mateusz. Z. Brela, Marek Boczar, Marek J. Wójcik, Harumi Sato, Takahito Nakajima, Yukihiro Ozaki	The Born - Oppenheimer Molecular Simulations of Infrared Spectra of Crystalline Poly-(R)-3-hydroxybutyrate with Analysis of Weak C-H…O=C Hydrogen Bonds	*Chem. Phys. Lett.*	**678**	112-118	2017.4.13
Mengfan Wang, Sanpon Vantasin, Jinping Wang, Harumi Sato, Jianming Zhang, and Yukihiro Ozaki	Distribution of polymorphic crystals in the ring-banded spherulites of poly(butylene adipate)studied using high-resolution raman imaging	*Macromolecules*	**50**	3377-3387	2017.4.13
Hotsumi Iwasaki, Madoka Nakamura, Nozomu Komatsubara, Makoto Okano, Masayoshi Nakasako, Harumi Sato, and Shinichi Watanabe	Controlled Terahertz Birefringence in Stretched Poly(lactic acid) Films Investigated by Terahertz Time-Domain Spectroscopy and Wide-Angle X-ray Scattering	*J. Phys. Chem. B*	**121**	6951–6957	2017.6.16
Morihisa Terasaki, Khasanah, Yukihiro Ozaki, Isao Takahashi, Harumi Sato	Study on phase separation in an ultra-thin poly(methyl methacrylate)/poly(4-vinyl phenol) film by infrared reflection absorption spectroscopy	*Polymer*	**135**	69-75	2018
Dian Marlina, Harumi Sato, Hiromichi Hoshina, and Yukihiro Ozaki	Intermolecular Interactions of Poly(3-hydroxybutyrate-co-3-hydroxyvalerate) (P(HB-co-HV)) with PHB-Type Crystal Structure and PHV-Type Crystal Structure Studied by Low-Frequency Raman and Terahertz Spectroscopies	*Polymer*	**135**	331-337	2017.12.11
Chihiro Funaki, Shigeki Yamamoto, Hiromichi Hoshina, Yukihiro Ozaki, and Harumi Sato	Three different kinds of weak C-H···O=C inter- and intramolecular interactions in poly(ε-caprolactone) studied by using terahertz spectroscopy, infrared spectroscopy and quantum chemical calculations	*Polymer*	**137**	245-254	2018.1.9
Seika Tatsuoka, Harumi Sato	Stress-induced crystal transition of poly(butylene succinate) studied by terahertz and low-frequency Raman spectroscopy and quantum chemical calculation	*Spectrochimica Acta Part A*		in press	2018.5
Mateusz. Z. Brela, Marek J. Wójcik, Marek Boczar, Erika Onishi, Harumi Sato, Takahito Nakajima, and Yukihiro Ozaki	Study of Hydrogen Bond Dynamics in Nylon 6 Crystals Using IR Spectroscopy and Molecular Dynamics Focusing on the Differences Between α and γ Crystal Forms	*Int. J. Quantum Chem.*		e25595	2018.2.5
Krzysztof B. Bec, Yusuke Morisawa, Kenta Kobashi, Justyna Grabska, Ichiro Tanabe, Erika Tanimura, Harumi Sato, Marek J. Wójcik and Yukihiro Ozaki	Rydberg transitions as a probe for structural changes and phase transition at polymer surfaces: an ATR-FUV-DUV and quantum chemical study of poly(3-hydroxybutyrate) and its nanocomposite with graphene	*Phys. Chem. Chem. Phys.*	**20**	8859-8873	2018.2.21
Xue Lan, Tomoyuki Mochida, Yusuke Funasako, Kazuyuki Takahashi, Takahiro Sakurai, and Hitoshi Ohta	Thermochromic Magnetic Ionic Liquids from Cationic Nickel(II) Complexes Exhibiting Intramolecular Coordination Equilibrium	*Chem. Eur. J.*	**23**	823-831	2016.11.2
T. Okamoto, H. Takahashi, E. Ohmichi, H. Ohta	Force-detected ESR Measurements in a Terahertz Range up to 0.5 THz and Application to Hemin	*Appl. Magn. Reson.*	**48**	435-444	2017.3.24
Tadyszak K, Rudowicz C, Ohta H, Sakurai T	Electron magnetic resonance data on high-spin Mn(III; S=2) ions in porphyrinic and salen complexes modeled by microscopic spin Hamiltonian approach	*J Inorg Biochem.*	**175**	36-46	2017.10

T. Sakurai, S. Okubo, H. Ohta	High-field/high-pressure ESR	*J. Mag. Res.*	**280**	3-9	2017.7
H. Takahashi, K. Ishimura, T. Okamoto, E. Ohmichi, H. Ohta	New Method for Torque Magnetometry Using a Commercially Available Membrane-Type Surface Stress Sensor	*J. Phys. Soc. Jpn.*	**86**	063002/1-4	2017.8.16
M. Kozanecki, C. Rudowicz, H. Ohta, T. Sakurai	High-frequency EMR data for Fe^{2}+ (S=2) ions in natural and synthetic forsterite revisited - Fictitious spin S'=1 versus effective spin S=2 approach	*Journal of Alloys and Compounds*	**726**	1226-1235	2017.12.5
M. Zajac, C. Rudowicz, H. Ohta, T. Sakurai	Spectroscopic and magnetic properties of Fe^{2+} ($3d^6$; S = 2) ions in Fe $(NH_4)_2(SO_4)_26H_2O$ – Modeling zero-field splitting and Zeeman electronic parameters by microscopic spin Hamiltonian approach	*J. Magn. Magn. Mat.*	**449**	94–104	2018.3.1
S. Murata, K. Takahashi, T. Sakurai, H. Ohta	Single-crystal-to-single-crystal transformation in hydrogen-bond- induced high-spin pseudopolymorphs from protonated cation salts with a p-extended spin crossover Fe(III) complex anion	*Polyhedron*	**136**	170-175	2017.11.4
S. Okubo, H. Ohta, T. Ijima, T. Yamasaki, W. Zhang, S. Hara, S. Ikeda, H. Oshima, M. Takahashi, K. Tomiyasu and T. Watanabe	THz ESR study of Spinel Compound $GeCo_2O_4$	*Z. Phys. Chem.*	**231**	827-837	2017.1
T. Mochida, Y. Funasako, H. Kimata, T. Tominaga, T. Sakurai, H. Ohta	Valence control of ionic molecular crystals: effect of substituents on the structures and valence states of biferrocenium salts with fluoro tetracyanoquinodimethanides"	*Crystal Growth & Design*	**17**	6020-6029	2017.10.11
T. Okamoto, E. Ohmichi, S. Okubo, H. Ohta	Precise Determination of Zero-Field Splitting Parameters of Hemin by High-Field and High-Frequency Electron Paramagnetic Resonance	*J. Phys. Soc. Jpn.*	**87**	013702/1-4	2017.12.6
E. Matsuoka, A. Oshima, H. Sugawara, T. Sakurai, H. Ohta	Possible Frustration Effects on a New Antiferromagnetic Compound $Ce_6Pd_{13}Zn_4$ with the Octahedral Ce Sublattices	*J. Phys. Soc. Jpn.*	**87**	013705/1-4	2017.12.14
E. Ohmichi, T. Miki, H. Horie, T. Okamoto, H. Takahashi, Y. Higashi, S. Itoh, H. Ohta	Mechanically detected terahertz electron spin resonance using SOI-based thin piezoresistive microcantilevers	*J. Mag. Res.*	**287**	41-46	2017.12.20
T. Mochida, M. Ishida, T. Tominaga, K. Takahashi, T. Sakurai, H. Ohta	Paramagnetic ionic plastic crystals containing the octamethylferrocenium cation: counteranion dependence of phase transitions and crystal structures	*J. Phys. Chem. Chem Phys.*	**20**	3019-3028	2017.5.23
T. Sakurai, Y. Hirao, K. Hijii, S. Okubo, H. Ohta, Y. Uwatoko, K. Kudo, Y. Koike	Direct Observation of the Quantum Phase Transition of $SrCu_2(BO_3)_2$ by High-Pressure and Terahertz Electron Spin Resonance	*J. Phys. Soc. Jpn.*	**87**	033701/1-4	2018.2.1
K. Takahashi, M. Okai, T. Mochida, T. Sakurai, H. Ohta, T. Yamamoto, Y. Einaga, Y. Shiota, K. Yoshizawa, H. Konaka, A. Sasaki	Contribution of Coulomb Interactions to a Two-Step Crystal Structure Phase Transformation Coupled with a Significant Change in Spin Crossover Behavior for a Series of Charged Fe^{II} Complexes from 2,6-Bis(2-methylthiazol-4-yl)pyridine	*Inorg. Chem.*	**57**	1277-1287	2018.1.8

Takahashi H, Ishimura K, Okamoto T, Ohmichi E, Ohta H.	Force- and torque-detection of high frequency electron spin resonance using a membrane-type surface-stress sensor.	*Rev. Sci. Intrum.*	**89**	036108/1-3	2018.3
T. Okamoto, T. Sakurai, E. Ohmichi, H. Ohta	Application of a high-frequency ESR technique using a SQUID magnetometer to a model complex of hemoproteins	*J. Jpn. Soc. Infrared Science & Technology*	**27**(1)	56-64	2017.8
T. Kohmoto, T. Moriyasu, S. Wakabayashi, H. Jinn, M. Takahara, and K. Kakita	Observation of Ultrafast Magnon Dynamics in Antiferromagnetic Nickel Oxide by Optical Pump-Probe and Terahertz Time-Domain Spectroscopies	*J. Infrared Milli. Terahz. Waves*	**39**	77-92	2017.9.25

Invited Talks (domestic and international) 招待講演(国内および国際研究集会)

発表者氏名	開催時期	開催地	plenary or invite	学会名	講演題目
小堀康博 Y. Kobori	2017.6. 25-30	幕張メッセ	invite	34th International Conference of Photopolymer Science and Technology Materials & Processes for Advanced Microlithography, Nanotechnology and Phototechnology	Time Resolved EPR Study on Photoinduced Charge-Separations in Thin Films of Thiophene-Thiazolothiazole Copolymer
	2017.5. 28 –6.1	New Orleans, USA	invite	231st ECS Meeting	Time-Resolved EPR Study on Charge Dynamics of Electron-Hole Pairs in Lead Iodide Perovskite Thin Film
	2017.6. 18 – 21,	淡路島	invite	5th Awaji International Workshop on "Electron Spin Science & Technology: Biological and Materials Science Oriented Applications" (5th AWEST 2017)	Electron spin polarization imaging applied to primary charge separation in the PSII
	2017.9. 17-21	Schluchsee, Germany	invite	Spin Chemistry Meeting 2017	Electron Spin Polarization Imaging of Photoinduced Primary Charge-Separated States in PSII
	2017.11 .12-15	東京	invite	第四回森野デスカッション	光合成初期反応の電子スピン画像解析
	2017.8. 25	千葉	invite	第 30 回生物無機化学夏季セミナー	時間分解電子スピン共鳴法による生体分子機能の解明
	2017.8. 31-9.2	淡路島	invite	11th Japanese-Russian Workshop on Open Shell Compounds and Molecular Spin Devices	Time-Resolved EPR Study on Photoinduced Charge-Transfer Trap States in Thiophene-Thiazolothiazole Copolymer Films
	2018.2. 4－6	石川	invite	タンタル酸ナトリウム光触媒のダイナミズムに関する研究会 2018	Motion and density distribution of photocarriers generated in $NaTaO_3$ photocatalyst
立川貴士 T. Tachikawa	2017.6. 17	福岡	invite	第 38 回 光化学若手の会	１分子・粒子レベルで観るマテリアルサイエンス
	2017.11 .6	神戸	invite	Kobe Mini-Symposium on Exciton and Charge Dynamics	Dynamics of Photogenerated Charges and Ions in Organolead Halide Perovskites
	2017.12 .11	仙台	invite	2017 年度 高分子・ハイブリッド材料研究センター（PHyM）若手フォーラム	有機無機ハイブリッドペロブスカイトの単一粒子発光観測
	2017.12 .26	大阪	invite	大阪大学産業科学研究所講演会	ハロゲン化鉛ペロブスカイトにおける光生成電荷とイオンのダイナミクス

富永圭介 K. Tominaga	2017.7. 23-28	Wisła, Poland	invite	8th International Discussion Meeting on Relaxations in Complex Systems	Broadband Dielectric Spectrocopy from MHz to THz on Proteins; Comaprison between Globular Proteins and Membrane Proteins
	2017.7. 31-8.4	USA	invite	Telluride Science Research Center Vibrational Dynamics	Dynamics of water, aqueous solutions, and proteins studied by 2DIR and broadband dielectric spectroscopy
	2017.11 .2-4	Hyderabad, India	plenar y	DAE-BRNS Theme Meeting on Ultrafast Science 2017	Dynamics of water, aqueous solutions, and proteins studied by 2DIR and broadband dielectric spectroscopy
	2017.11 .9-10	Tokyo Institute of Technology	invite	2nd International Symposium on Biomedical Engineering	Terahertz Spectroscopy and Theoretical Calculation on Biologically Important Molecules and Pharmaceutical Molecules
	2017.11 .13	IMS, Okazaki	invite	Workshop on Reaction and Structural Dynamics in Condensed Phases	Dynamics of water, aqueous solutions, and proteins studied by 2DIR and broadband dielectric spectroscopy
	2018.1. 3-7	Mumbai, India	invite	14th DAE-BRNS Biennial Trombay Symposium on Radiation & Photochemistry (TSRP-2018)	Broadband Dielectric Spectroscopy on Proteins and Lipid Bilayers from sub-GHz to THz
	2018.1. 7-10	Hong Kong	invite	10th Asian Conference on Ultrafast Phenomena	Broadband Dielectric Spectroscopy on Proteins and Lipid Bilayers from sub-GHz to THz
	2018.2. 27-3.2	Bangalore, India	invite	90 Years of Raman Effect: Current Status and Future Directions	Vibrational Frequency Fluctuations of Solutes in Water Studied by 2DIR Spectroscopy
太田薫 K. Ohta	2017.11 .6	神戸	invite	Kobe Mini-Symposium on Exciton and Charge Dynamics	Charge Carrier Dynamics in Porphyrin-Based Organic Thin Films Studied by Time-Resolved Terahertz Spectroscopy
Feng Zhang	2017.2. 22	福井	invite	FIR Center seminar	THz Spectroscopy of Molecular Crystals: Mode Assignment and Applications in Crystallography
山本直樹 N. Yamamoto （理学研究科）	2017.2. 22	福井	invite	FIR Center seminar	Temperature and Hydration Dependence of Protein Dynamics Studied by Broadband Dielectric Spectroscopy
奥田真紀 M. Okuda	2018.1. 3-7	Mumbai, India	invite	14th DAE-BRNS Biennial Trombay Symposium on Radiation & Photochemistry (TSRP-2018)	Vibrational Frequency Fluctuations of Solute in Water Studied by Two-Dimensional Infrared Spectroscopy
	2018.1. 7-10	Hong Kong	invite	10th Asian Conference on Ultrafast Phenomena	Vibrational Frequency Fluctuations of Solute in Water Studied by Two-Dimensional Infrared Spectroscopy
佐藤春実 H. Sato (人間発達環境学研究科)	2017.6. 11-16	Victoria, BC, Canada	invite	ICAVS2017	Intermolecular Interaction and Higher-Order Structure of Biodegradable Polyester Studied by Terahertz Spectroscopy
	2017.7. 8	仙台	invite	第 45 回東北地区高分子若手研究会夏季ゼミナール	高分子分光法による高分子の高次構造の研究

太田仁 H. Ohta	2017.5. 12-14	八王子	invite	第 13 回 ESR 入門セミナー	超入門
	2017.5. 12-14	八王子	invite	第 13 回 ESR 入門セミナー	スペクトル解析 I(固体)
	2017.5. 23-26	Peterhof, Russia	invite	Dzyaloshinskii-Moriya Interaction and Exotic Spin Structures	Determination of DMI in Kagome Lattice Antiferromagnet Cr-Jarosite by High-Frequency ESR
	2017.6. 18-21	淡路島	invite	5th Awaji International Workshop on "Electron Spin Science & Technology: Biological and Materials Science Oriented Applications" (5th AWEST 2017)	Recent Status of Multi-Extreme THz ESR in Kobe
	2017.7. 7	岡崎	invite	第 15 回 ESR 夏の学校	電子スピン共鳴（ESR）序論
	2017.7. 16-22	West Virginia, USA	invite	International Conference on Electron Paramagnetic Resonance Spectroscopy and Imaging of Biological Systems (EPR2017)	Developments of Multi-Extreme THz ESR:towards the biological application
	2017.8. 9-16	Gothenburg, Sweden	invite	28th International Conference on Low Temperature Physics	Observation of high pressure phase in Shastry-Sutherland Model Substance $SrCu_2(BO_3)_2$ by high puressure THz ESR
	2017.9. 25-29	Kazan, Russia	invite	Modern Development of Magnetic Resonance 2017 (MDMR 2017)	Multi-Extreme THz ESR: Developments and Future Biological Applications
	2018.3. 15	Frankfurt am Main, Germany	invite	Seminar at Goethe Universitat	Recent Developments of Multi-Extreme THz ESR in Kobe
	2018.3. 19	Dresden, Germany	invite	Quantum Matter Colloquium in IFW Dresden	Direct Observation of the Quantum Phase Transitions of $SrCu_2(BO_3)_2$ by High-Pressue and Terahertz Electron Spin Resonance
大道英二 E. Ohmichi (理学研究科)	2017.10 .4-6	Frascati, Italy	invite	8th International THz-Bio workshop 2017 (THz-Bio 2017)	Mechanically Detected Electron Paramagnetic Resonance Spectroscopy in the Terahertz Region
	2017.10 .19	名古屋	invite	第 5 回豊田理研ワークショップ「スピン秩序の動的光制御」	機械的検出によるテラヘルツ電子スピン共鳴法の開発
高橋英幸 H. Takahashi (先端融合研究環)	2018.3. 5-7	つくば	invite	MANA International Symposium 2018	Torque magnetometry using a membrane-type surface stress sensor
河本敏郎 T. Kohmoto (理学研究科)	2017.10 .19-20	名古屋	invite	第 5 回豊田理研ワークショップ「スピン秩序の動的光制御」	酸化物磁性体における電場誘起磁化のダイナミクス

Presentation at conferences (international and domestic) **一般講演**

発表者氏名	開催時期	開催地	plenary or invite	学会名	講演題目
笠原俊二 S. Kasahara	2017.7. 14-15	姫路	poster	International Symposium on "Diversity of Chemical Reaction Dynamics"	Hyperfine-resolved high-resolution laser spectroscopy of $^{14}NO_2$ in 14500－16800 cm^{-1}
	2017.8. 27-9.1	葉山	oral	34th International Symposium on Free Radicals	Rotationally Resolved High-Resolution Laser Spectroscopy of B-X Transition of Nitrate Radical
	2017.8. 27-9.1	葉山	poster	34th International Symposium on Free Radicals	Rotationally-Resolved High-Resolution Laser Spectroscopy of $S_1 \leftarrow S_0$ transition of Fluorene
	2017.9. 15-18	仙台	poster	第 11 回分子科学討論会	NO_2 ラジカルの 595-686 nm 領域の高分解能レーザー分光
	2018.3. 19-20	つくば	oral	第 18 回分子分光研究会	フルオレンおよびカルバゾールの $S_1 \leftarrow S_0$ 遷移の高分解能レーザー分光
小堀康博 Y. Kobori	2017.5. 28-6.1	New Orleans, USA	oral	231st ECS Meeting	Geometries and Dynamics of Photoinduced Electron-Hole Pairs in Polyhexylthiophene-Fullerene Systems
	2017.9. 5-9.7	仙台	oral	2017 年光化学討論会	Electron tunneling route of photoinduced primary charge-separated state in the PSII studied by electron spin polarization imaging method
	2017.11 .2-11.4	東京	oral	第 56 回電子スピンサイエンス学会年会（SEST2017）	電子スピン分極イメージング法によるクリプトクロム光電荷分離状態の立体構造解析
立川貴士 T. Tachikawa	2017.6. 30	大阪	oral	第 36 回 光がかかわる触媒化学シンポジウム	チタン酸ストロンチウムメソ結晶の合成と水分解光触媒への応用
	2017.9. 4	仙台	oral	2017 年光化学討論会	チタン酸ストロンチウムメソ結晶光触媒における特異な電荷移動挙動
	2017.11 .22	滋賀	oral	第 36 回 固体・表面光化学討論会	タンタル酸ナトリウム光触媒の発光挙動におけるドーピングの効果
富永圭介 K. Tominaga	2017.6. 4-9	Sendai, Japan	oral	6th International Conference on Photoinduced Phase Transitions	Vibrational dynamics of the CO stretching of 9-fluorenone and its derivatives studied by visible-pump and infrared-probe spectroscopy
太田薫 K. Ohta	2017.6. 4-9	Sendai, Japan	poster	6th International Conference on Photoinduced Phase Transitions	Charge Carrier Dynamics in Porphyrin Based Organic Semiconductors Studied by Time-Resolved Terahertz Spectroscopy
	2017.6. 4-9	Sendai, Japan	poster	6th International Conference on Photoinduced Phase Transitions	Development of Wavefront Shaping Technique for Ultrashort Optical Pulses
	2017.9. 15-18	仙台	oral	第 11 回分子科学討論会	時間分解テラヘルツ分光法によるポルフィリン系有機薄膜の電荷キャリアの生成と緩和過程の研究
佐藤春実 H. Sato	2017.5. 29-31	千葉	poster	第 66 回高分子年次大会	テラヘルツ分光法を用いた太陽光パネル封止材の紫外線劣化評価

	2017.9.18	Kiel, Germany	oral	Kobe-Kiel bilateral workshop	Terahertz spectroscopy and its applications in polymers
太田仁 H. Ohta	2017.4.2-6	Oxford, UK	oral	50th Annual International Meeting of the Electron Spin Resonance Group of the Royal Society of Chemistry	Multi-Extreme THz ESR: Developments and Future
	2017.7.23-28	Quebec, Canada	oral	20th meeting of International Society of Magnetic Resonance (20th ISMAR)	Development of Multi-Extreme THz ESR: Present and Future
	2017.10.26-27	大阪	oral	第 27 回（平成 29 年度）日本赤外線学会研究発表会	多重極限 THz ESR の現状と展望
	2017.11.2-4	東京	oral	第 56 回電子スピンサイエンス学会年会（SEST2017)	多重極限 THz ESR の開発とその展望
	2017.11.29-30	つくば	oral	第 13 回強磁場フォーラム総会	ユーザーから見た強磁場施設
	2017.11.29-30	つくば	Poster	第 13 回強磁場フォーラム総会	強磁場・高圧・低温による多重極限 THz ESR による物性研究
	2017.12.4-5	大阪	oral	第 12 回量子スピン系研究会	多重極限下測定と測定技術の進展
大久保晋 S. Okubo	2017.8.9-16	Gothenburg, Sweden	poster	28th International Conference on Low Temperature Physics	High-Field ESR study of S=1/2 frustrated J_1-J_2 chain $NaCuMoO_4(OH)$ as candidate substance for spin nematic
	2017.9.21-24	岩手	poster	日本物理学会　2017 年秋季大会	トポロジカル絶縁体 Bi_2Se_3 のサイクロトロン共鳴
	2017.9.21-24	岩手	oral	日本物理学会　2017 年秋季大会	S=1/2 歪んだダイアモンド鎖化合物（$Cu_3(OH)_2(CH_3CO_2)_2(H_2O)_xX_y$)のサブミリ波 ESR 測定 II
	2017.11.29-30	つくば	poster	強磁場コラボラトリーが拓く未踏計測領域への挑戦と物質・材料科学の最先端	スピンネマチック候補物質 S=1/2 擬１次元 J_1-J_2 フラストレート磁性体 $NaCuMoO_4(OH)$の磁場中配向試料による強磁場 ESR 測定
	2017.12.4-5	大阪	oral	第 12 回量子スピン系研究会	S=1/2 1 次元量子スピン鎖 $MCuMoO_4(OH)$(M-K, Na)の強磁場 ESR 測定
	2018.3.7	福井	oral	平成 29 年度福井大学遠赤外領域開発センター共同研究成果報告会	磁気キラル対称性の破れた磁性体の磁気異方性の研究
	2018.3.22-25	東京	poster	日本物理学会　第 73 回年次大会（2018 年）	S=1/2 反強磁性鎖 $KCuMoO_4(OH)$の高周波 ESR 測定 II
高橋英幸 H. Takahashi (先端融合研究環)	2017.9.21-24	岩手	oral	日本物理学会　2017 年秋季大会	magnet-on-cantilever 配置による力検出型テラヘルツ ESR 測定
	2017.9.25	大阪	oral	第四回西日本強磁場科学研究会	メンブレン型共振器を用いた磁気測定および磁気共鳴測定
	2017.11.2-4	東京	oral	第 56 回電子スピンサイエンス学会年会（SEST2017)	メンブレン型表面応力センサーを用いた力/トルク検出 ESR

	2017.11.29-30	つくば	oral	強磁場コラボラトリーが拓く未踏計測領域への挑戦と物質・材料科学の最先端	メンブレン型表面応力センサーを用いた磁気測定
	2018.3.22-25	東京	poster	日本物理学会　第 73 回年次大会（2018 年）	凍結溶液試料の力検出型高周波 ESR 測定法の開発
櫻井敬博 T. Sakurai (研究基盤センター)	2017.9.21-24	岩手	poster	日本物理学会　2017 年秋季大会	三角格子反強磁性体 $CsCuCl_3$ の圧力下 THz-ESR 測定 III
	2017.10.26-27	大阪	oral	第 27 回（平成 29 年度）日本赤外線学会研究発表会	テラヘルツ領域における高圧力下 ESR 装置の開発と応用
	2017.11.29-30	つくば	oral	強磁場コラボラトリーが拓く未踏計測領域への挑戦と物質・材料科学の最先端	強磁場高圧下テラヘルツ ESR 装置の開発と応用
	2018.3.22-25	東京	oral	日本物理学会　第 73 回年次大会（2018 年）	三角格子反強磁性体 $CsCuCl_3$ のプラトー領域における圧力下強磁場 ESR
原茂生 S. Hara (研究基盤センター)	2017.12.4-5	大阪	oral	第 12 回量子スピン系研究会	新奇量子スピン系の探索
齋藤佑 Y. Saito (研究基盤センター)	2017.11.2-4	東京	oral	第 56 回電子スピンサイエンス学会年会（SEST2017)	圧力下ヘミンの Thz 領域における多周波数強磁場 ESR

Presentation by Graduate Students and Postdocs 院生、ポストドクの学会発表

指導教員	発表者氏名	学年	時期	学会名	講演題目
笠原俊二 S. Kasahara	黒田真司	M2	2017.5.19	第 17 回分子分光研究会	単一モード紫外レーザーによるフルオレンの高分解能分光
	黒田真司	M2	2017.6.7-9	33rd Symposium on Chemical Kinetics and Dynamics	High-resolution laser spectroscopy of the S_1-S_0 transition of fluorene
	平田通啓	M2	2017.6.7-9	33rd Symposium on Chemical Kinetics and Dynamics	Hyperfine interaction in the excited electronic state of NO_2 radical
	黒田真司	M2	2017.7.14-15	International Symposium: Recent Progress in Molecular Spectroscopy and Dynamics	Rotationally-Resolved High-Resolution Laser Spectroscopy of Fluorene
	黒田真司	M2	2017.9.15-18	第 11 回分子科学討論会	分子線を用いたフルオレンの S_1-S_0 遷移の高分解能レーザー分光
小堀康博 Y. Kobori	江間文俊	D2	2017.6.18 – 21	5th Awaji International Workshop on "Electron Spin Science & Technology: Biological and Materials Science Oriented Applications" (5th AWEST 2017)	Charge Carrier Dynamics of $CH_3NH_3PbBr_{3-x}I_x$ with Hetero-Band StructuresTime-resolved EPR Study on Antiaromatic Excited Triplet State of [28]Hexaphyrin with Twisted Möbius Conformation
	江間文俊	D2	2017.6.18 – 21	5th Awaji International Workshop on "Electron Spin Science & Technology: Biological and Materials Science Oriented Applications" (5th AWEST 2017)	Time-resolved EPR Study on Photoinduced Electron Spin Polarization and Dynamics of Radicals at Bilayer Interface
	江間文俊	D2	2017.7.15	第 21 回 ESR フォーラム研究会 2017	シロキ基を有する室温リン光発性有機結晶の三重項状態に対する時間分解 EPR 観測
	山本雄大	M2	2017.7.15	第 21 回 ESR フォーラム研究会 2017	TREPR 法によるチオフェン-チアゾロチアゾールポリマー簿膜に生成する光誘起キャリアトラップ状態の観測
	見延玲奈	M2	2017.7.15	第 21 回 ESR フォーラム研究会 2017	PSII 反応中心の光電荷分離と励起子生成に対する励起波長依存性
	長嶋宏樹	PD	2017.9.5-7	2017 年光化学討論会	Time-resolved and pulsed electron paramagnetic resonance study on the singlet-fission materials
	江間文俊	D2	2017.9.5-7	2017 年光化学討論会	時間分解 EPR 法による室温リン光発光性有機包接結晶の励起三重項状態の電子構造
	山本雄大	M2	2017.9.5-7	2017 年光化学討論会	Time-Resolved EPR Study on Photoinduced Charge-Transfer Trap State in Thiophene-Thiazolothiazole Copolymer Film
	見延玲奈	M2	2017.9.5-7	2017 年光化学討論会	PSII 反応中心の光電荷分離と励起子生成に対する励起波長依存性
	濱田美里	M1	2017.9.5-7	2017 年光化学討論会	アフリカツメガエル由来クリプトクロムに生成する光電荷分離状態の電子的相互作用
	長嶋宏樹	PD	2017.9.19-21	第 55 回日本生物物理学会年会	高等植物の光化学系 II における効率的な電荷分離反応のメカニズム/The mechanism of efficient charge separation reaction in photosystem II of higher plants
	江間文俊	D2	2017.10.17-19	第 7 回 CSJ 化学フェスタ 2017	時間分解 EPR 法による室温リン光発光性有機包接結晶の励起三重項状態の電子構造

	長嶋宏樹	PD	2017.11.2-11.4	第 56 回電子スピンサイエンス学会年会（SEST2017）	ペンタセン・テトラセン誘導体における一重項分裂により生成した五重項状態の観測
	江間文俊	D2	2017.11.2-11.4	第 56 回電子スピンサイエンス学会年会（SEST2017）	時間分解 EPR 法による室温リン光発光性有機包接結晶の三重項電荷移動状態におけるゲスト分子依存性
	山本雄大	M2	2017.11.2-11.4	第 56 回電子スピンサイエンス学会年会（SEST2017）	TREPR 法によるチオフェン-チアゾロチアゾールポリマー薄膜に生成する光誘起キャリアトラップ状態の観測
	見延玲奈	M2	2017.11.2-11.4	第 56 回電子スピンサイエンス学会年会（SEST2017）	PSII 反応中心の光電荷分離と励起子生成に対する励起波長依存性
	濱田美里	M1	2017.11.2-11.4	第 56 回電子スピンサイエンス学会年会（SEST2017）	アフリカツメガエル由来クリプトクロムに生成する光電荷分離状態の電子的相互作用
立川貴士 T. Tachikawa	狩俣出	D1	2017.6.17	第 38 回 光化学若手の会	ペロブスカイトナノ粒子の単一粒子発光観測
	狩俣出	D1	2017.6.17	第 7 回 CSJ 化学フェスタ 2017	有機無機ペロブスカイトのハロゲン交換反応における過渡種生成と電荷捕集のその場観察
	狩俣出	D1	2017.9.4	2017 年光化学討論会	Slow charge transfer process over a few nanoseconds in heterostructured $CH_3NH_3PbBr_{3-x}I_x$
	水谷晟吾	M1	2017.9.5	2017 年光化学討論会	深紫外蛍光顕微鏡による $NaTaO_3$ 光触媒の発光観測
	村上雄太	M1	2017.9.5	2017 年光化学討論会	顕微分光法を用いた二酸化チタンメソ結晶の光機能性評価
	狩俣出	D1	2017.10.18	第 7 回 CSJ 化学フェスタ 2017	有機無機ペロブスカイトのハロゲン交換反応における過渡種生成と電荷捕集のその場観察
	木村優季	M1	2017.10.19	第 7 回 CSJ 化学フェスタ 2017	有機金属ハロゲン化物ペロブスカイトにおける光反応挙動の単一粒子解析
	櫻井学	M2	2017.11.2	第 56 回 電子スピンサイエンス学会年会 (SEST2017)	光誘起電子移動反応における磁場効果を利用した新規蛍光イメージング法の開発
富永圭介 K. Tominaga	Feng Zhang	PD	2017.5	3rd annual conference on THz science and technology	Terahertz Vibrational Spectroscopy in Molecular Crystalline Systems
	Feng Zhang	PD	2017.8	15th annual chemical dynamics conference	Terahertz Vibrational Spectroscopy in Molecular Crystalline Systems
	奥田真紀	PD	2017.7	XVIIIth Time Resolved Vibrational Spectroscopy	Hydrogen-bond dynamics of 9-fluorenone derivatives in water probed by 2D-IR spectroscopy
	奥田真紀	PD	2017.9	第 11 回分子科学討論会	二次元赤外分光法による水溶液中における 9-フルオレノン誘導体の振動ダイナミクスの解明
	奈良隆史	M2	2017.9.15-18	第 11 回分子科学討論会	広帯域分光法及び分子動力学シミュレーションによるグアニジウムイオン及びテトラメチルアンモニウムイオンの水和水のダイナミクス
	門村友	M1	2017.9.15-18	第 11 回分子科学討論会	広帯域誘電分光法によるホスホリルコリン基を有する脂質の動的挙動に及ぼす水和の影響
	平松優一	M1	2017.9.15-18	第 11 回分子科学討論会	光ポンプ-テラヘルツプローブ分光法によるバルクヘテロ接合型有機半導体における電荷キャリアダイナミクス

	奈良隆史	M2	2017.10.28	第 8 回サイエンスフロンティア研究発表会	グアニジウムイオン及びテトラメチルアンモニウムイオンの水和水のダイナミクスに関する分光学的・理論的研究
	門村友	M1	2017.10.28	第 8 回サイエンスフロンティア研究発表会	広帯域誘電分光法によるホスホリルコリン基を有する脂質の動的挙動に及ぼす水和の影響
	門村友	M1	2017.12.21	若手フロンティア研究会 2017	広帯域誘電分光法によるリン脂質の動的挙動に及ぼす水和の影響
	平松優一	M1	2017.12.21	若手フロンティア研究会 2017	光ポンプ-テラヘルツプローブ分光法によるバルクヘテロ接合型有機半導体における電荷キャリアの挙動
	平松優一	M1	2018.1.23-24	スーパーコンピューターワークショップ 2017「機能性材料設計への最新の計算科学アプローチ」	光ポンプ-テラヘルツプローブ分光法によるバルクヘテロ接合型有機半導体における電荷キャリアのダイナミクス
佐藤春実 H. Sato	中村萌	M2	2017.5.29-31	第 66 回高分子年次大会	ラマン・テラヘルツ分光法を用いたステレオコンプレックス型ポリ乳酸の紫外線劣化評価
	長濱朋輝	M1	2017.5.29-31	第 66 回高分子年次大会	低波数ラマン及びテラヘルツ分光法によるコラーゲン及びコラーゲンモデル化合物の構造変化
	長濱朋輝	M1	2017.7.11-16	ICAVS2017	Thermal Denaturation and structural changes of collagen model peptide studied by low frequency Raman and THz spectroscopy
	中村萌	M2	2017.7.14	第 63 回高分子研究発表会（神戸）	テラヘルツ分光法によるステレオコンプレックス型ポリ乳酸の紫外線劣化過程に関する研究
	舟木千尋	M2	2017.7.14	第 63 回高分子研究発表会（神戸）	テラヘルツ分光法によるポリカプロラクトンの紫外線劣化と高次構造の相関
	舟木千尋	M2	2017.9.20-22	第 66 回高分子討論会	テラヘルツ分光法を用いたポリカプロラクトンの高次構造の研究
	中村萌	M2	2017.9.20-22	第 66 回高分子討論会	テラヘルツ分光法を用いたステレオコンプレックス型ポリ乳酸の結晶構造変化に関する研究
	辰岡星佳	M2	2017.9.20-22	第 66 回高分子討論会	THz 及び赤外分光法を用いた PBS(ポリブチレンサクシネート)の高次構造の研究
	鈴木修平	M2	2017.9.20-22	第 66 回高分子討論会	振動分光法を用いたポリヒドロキシブタン酸共重合体の結晶化挙動に及ぼす添加剤の影響
	長濱朋輝	M1	2017.9.20-22	第 66 回高分子討論会	低波数ラマン分光法におけるコラーゲンモデル化合物の高次構造変化
	Dian Marlina	D1	2017.9.20-22	第 66 回高分子討論会	Study of Higher Ordered Structure of Biodegradable Polymer by Terahertz and Low-Frequency Raman Spectroscopies
	舟木千尋	M2	2017.12.4-6	テラヘルツ科学の最先端 Ⅳ	テラヘルツ分光法を用いたポリカプロラクトンの水素結合の役割の解明
	岡崎なつ実	B4	2017.12.4-6	テラヘルツ科学の最先端 Ⅳ	ポリジオキサノン（PDS）のテラヘルツ分光法による分子間相互作用に関する研究
	山元優美子	B4	2017.12.4-6	テラヘルツ科学の最先端 Ⅳ	ポリエチレンテレフタレート及びポリブチレンテレフタレートの THz 分光法による高次構造の研究

	辰岡星佳	M2	2017.12.4-6	テラヘルツ科学の最先端 IV	低波数領域におけるポリブチレンサクシネート（PBS）の高次構造の研究
	Dian Marlina	D1	2017.12.4-6	テラヘルツ科学の最先端 IV	Higher Ordered Structure of Chitosan Polyethylere Glycol Blends Studied by Terahertz Spectroscopy
太田仁 H. Ohta	岡本翔	D2	2017.5.12-14	第 13 回 ESR 入門セミナー	研究講演I　マイクロカンチレバーを用いた高周波電子スピン共鳴法の開発とその生体関連物質への応用
	宮崎大輔	M2	2017.6.18-21	5th Awaji International Workshop on "Electron Spin Science & Technology: Biological and Materials Science Oriented Applications" (5th AWEST 2017)	Submillimeter and millimeter wave ESR measurements of S=1/2 distorted diamond chain compounds $(Cu_3(OH)_2(CH_3CO_2)_2(H_2O)_xX_y)$($X_y$=2,6-NP$(SO_3)_2$, 1,5-NP$(SO_3)_2$, Et$C_6H_4SO_3$)
	岡本翔	D2	2017.6.18-21	5th Awaji International Workshop on "Electron Spin Science & Technology: Biological and Materials Science Oriented Applications" (5th AWEST 2017)	In-plane magnetic anisotropy of hemin revealed by high-field and high-frequency electron spin resonance
	石村謙斗	M1	2017.6.18-21	5th Awaji International Workshop on "Electron Spin Science & Technology: Biological and Materials Science Oriented Applications" (5th AWEST 2017)	Development of force-detected high frequency ESR technique using a membrane-type surface stress sensor
	下城世那	M1	2017.9.21-24	日本物理学会　2017 年秋季大会	Co 正方格子の ESR 測定
	藤本達也	M1	2017.9.21-24	日本物理学会　2017 年秋季大会	波長可変テラヘルツ光源を用いた電子スピン共鳴法の開発
	石村謙斗	M1	2017.9.21-24	日本物理学会　2017 年秋季大会	メンブレン型ピエゾ抵抗センサーを用いた高周波 ESR 測定法の開発
	岡本翔	D2	2017.9.19-21	第 55 回日本生物物理学会年会	カンチレバーを用いた高感度多周波 EPR 測定法の開発とヘミンへの応用
	岡本翔	D2	2017.9.25	第四回西日本強磁場科学研究会	金属ポルフィリン錯体ヘミンの強磁場 ESR 測定
	宮崎大輔	M2	2017.9.25	第四回西日本強磁場科学研究会	S=1/2 歪んだダイアモンド鎖化合物 $(Cu_3(OH)_2(CH_3CO_2)(H_2O)_xX_y)$の強磁場 ESR 測定
	久保田創	M2	2017.9.25	第四回西日本強磁場科学研究会	S=1/2　反強磁性鎖 $KCuMoO_4(OH)$配向試料を用いた ESR 測定
	堀江秀和	M2	2017.9.25	第四回西日本強磁場科学研究会	カシミール力測定にむけた高感度力検出装置の開発
	大木瑛登	M2	2017.9.25	第四回西日本強磁場科学研究会	三角格子反強磁性体 $CsCuCl_3$ の圧力下磁化プラトー現象の起源解明

出口健太	M1	2017.9.25	第四回西日本強磁場科学研究会	微小磁気チップ付きマイクロカンチレバーの作製
石村謙斗	M1	2017.9.25	第四回西日本強磁場科学研究会	メンブレン型ピエゾ抵抗センサーを用いた角度回転高周波 ESR
藤本達也	M1	2017.9.25	第四回西日本強磁場科学研究会	波長可変光源を用いた磁場中テラヘルツ分光方の開発
下城世那	M1	2017.9.25	第四回西日本強磁場科学研究会	Co 正方格子反強磁性体の強磁場 ESR 測定
K. Benzid	PD	2017.9.25	第四回西日本強磁場科学研究会	High frequency ESR study of magnetic field inducted transition in powdered Co-substituted $BiFeO_3$
藤本達也	M1	2017.10.26-27	第 27 回（平成 29 年度）日本赤外線学会研究発表会	波長可変テラヘルツ光源を用いた磁場中分光法の開発
下城世那	M1	2017.10.26-27	第 27 回（平成 29 年度）日本赤外線学会研究発表会	Co 正方格子反強磁性体の THz ESR 測定
堀江秀和	M2	2017.10.26-27	第 27 回（平成 29 年度）日本赤外線学会研究発表会	Fabry-Perot 干渉計を用いたカシミール力測定装置の開発
石村謙斗	M1	2017.10.26-27	第 27 回（平成 29 年度）日本赤外線学会研究発表会	メンブレン型ピエゾ抵抗センサーを用いたミリ波領域 ESR 測定
出口健太	M1	2017.10.26-27	第 27 回（平成 29 年度）日本赤外線学会研究発表会	テラヘルツ磁気共鳴顕微鏡のための微小磁気チップ付きカンチレバーの開発
久保田創	M2	2017.10.26-27	第 27 回（平成 29 年度）日本赤外線学会研究発表会	S=1/2 反強磁性鎖 $KCuMoO_4(OH)$配向試料を用いた高周波 ESR 測定
大木瑛登	M2	2017.10.26-27	第 27 回（平成 29 年度）日本赤外線学会研究発表会	三角格子反強磁性体 $CsCuCl_3$ のテラヘルツ領域における圧力下 ESR 測定
岡本翔	D2	2017.10.26-27	第 27 回（平成 29 年度）日本赤外線学会研究発表会	金属ポルフィリン錯体ヘミンの THz-ESR 測定
宮崎大輔	M2	2017.10.26-27	第 27 回（平成 29 年度）日本赤外線学会研究発表会	S=1/2 歪んだダイアモンド鎖化合物（$Cu_3(OH)_2(CH_3CO_2)_2(H_2O)_xX_y$)のテラヘルツ ESR 測定
岡本翔	D2	2017.11.2-4	第 56 回電子スピンサイエンス学会年会（SEST2017)	強磁場・テラヘルツ領域におけるヘミンの精密 ESR 分光
岡本翔	D2	2017.12.21	若手フロンティア研究会 2017	強磁場・テラヘルツ領域におけるヘミンの ESR 研究
下城世那	M1	2017.12.21	若手フロンティア研究会 2017	Co 正方格子反強磁性体の ESR 測定
藤本達也	M1	2017.12.21	若手フロンティア研究会 2017	波長可変テラヘルツ光源を用いた磁場中 ESR 分光法の開発
石村謙斗	M1	2017.12.21	若手フロンティア研究会 2017	メンブレン型ピエゾ抵抗センサーを用いた高感度磁気測定

	堀江秀和	M2	2017.12.21	若手フロンティア研究会 2017	マイクロカンチレバーを用いた高感度力検出装置の開発
	宮崎大輔	M2	2017.12.21	若手フロンティア研究会 2017	有機ダイヤモンド鎖型反強磁性体の強磁場 ESR 測定
	出口健太	M1	2017.12.21	若手フロンティア研究会 2017	高感度磁気チップ付きマイクロカンチレバー
	大木瑛登	M2	2017.12.21	若手フロンティア研究会 2017	新しい圧力下強磁場 ESR 装置による $CsCuCl_3$
	久保田創	M2	2017.12.21	若手フロンティア研究会 2017	場の量子論で理解される励起モードの観測
	藤本達也	M1	2018.3.22-25	日本物理学会　第 73 回年次大会（2018 年）	波長可変テラヘルツ光源を用いた電子スピン共鳴法の開発 II
	下城世那	M1	2018.3.22-25	日本物理学会　第 73 回年次大会（2018 年）	幾何学的スピン構造をもつ反強磁性体の強磁場 ESR による研究
	岡本翔	D2	2018.3.22-25	日本物理学会　第 73 回年次大会（2018 年）	窒化シリコンナノメンブレンを用いた力検出テラヘルツ ESR 測定法の開発
河本敏郎 T. Kohmoto	蓮沼貴史	M2	2017.5.23-25	平成 29 年度日本分光学会年次講演会	YIG における電場誘起磁化
	疋田崚	M1	2017.5.23-25	平成 29 年度日本分光学会年次講演会	反強磁性体酸化クロムにおける電場誘起磁化
	川本憲生	M1	2017.5.23-25	平成 29 年度日本分光学会年次講演会	反強磁性体 Cr_2O_3 における電場誘起磁化のダイナミクス
	疋田崚	M1	2017.6.4-8	9th International School and Conference on Spintronics and Quantum Information Technology	Dynamics of the electric-field induced magnetization in antiferromagnetic chromium oxide: Faraday rotation measurement
	川本憲生	M1	2017.6.4-8	9th International School and Conference on Spintronics and Quantum Information Technology	Magnetic-field dependence of the coherent magnons in an antiferromagnet NiO
	蓮沼貴史	M2	2017.6.4-8	9th International School and Conference on Spintronics and Quantum Information Technology	Dynamics of the electric-field induced magnetization in YIG observed by Faraday rotation
	疋田崚	M1	2017.10.19-20	第 5 回豊田理研ワークショップ「スピン秩序の動的光制御」	反強磁性体酸化クロムにおける電場誘起磁化のダイナミクス
	蓮沼貴史	M2	2017.10.19-20	第 5 回豊田理研ワークショップ「スピン秩序の動的光制御」	YIG における電場誘起磁化
	疋田崚	M1	2017.10.28	第 8 回サイエンスフロンティア研究発表会	反強磁性体酸化クロムにおける電場誘起磁化
	蓮沼貴史	M2	2017.10.28	第 8 回サイエンスフロンティア研究発表会	YIG における電場誘起磁化

	疋田崚	M1	2017.12.4-5	第 22 回スピン工学の基礎と応用	反強磁性体酸化クロムにおける電場誘起磁化のダイナミクス
	疋田崚	M1	2017.12.8-9	第 28 回光物性研究会	反強磁性体 Cr_2O_3 における電場誘起磁化のダイナミクス
	蓮沼貴史	M2	2017.12.8-9	第 28 回光物性研究会	YIG における電場誘起磁化
	藤本恵輔	B4	2018.3.22-25	日本物理学会　第 73 回年次大会（2018 年）	YIG における電場誘起磁化
	谷口弘樹	B4	2018.3.22-25	日本物理学会　第 73 回年次大会（2018 年）	反強磁性体酸化クロムにおける電場誘起磁化のダイナミクス

Books **著書**

著者（共著者も含む）	書名	出版社名	ページ数	発行年

Other Publications **参考論文･記事･報告**

著者	タイトル	出版物名	巻・号・ページ	発行年
立川貴士	メソ結晶空間を利用した高効率光触媒の開発	月刊「化学工業」	68 巻 10 号 21-26	2017
立川貴士	チタン酸ストロンチウムメソ結晶光触媒を利用した光水素製造	太陽エネルギー	44 巻 1 号 33-40	2018
守安毅，笹島秀樹，河本敏郎，北原英明，谷正彦，熊倉光孝	光励起したシリコンにおけるテラヘルツパルスの伝播	電子情報通信学会技術研究報告(信学技報)	28 巻 291-294	2017.12
疋田崚，谷口弘樹，河本敏郎	反強磁性体 Cr_2O_3 における電場誘起磁化のダイナミクス	光物性研究会論文集	68 巻 10 号 21-26	2017
蓮沼貴史，藤本恵輔，河本敏郎	YIG における電場誘起磁化	光物性研究会論文集	44 巻 1 号 33-40	2018

Lecture to Public **講演、模擬授業など**

氏名	講演題目	集会名	日時	場所
河本敏郎	光と色の科学	出前授業	2017.5.31	西宮東高校
河本敏郎	光と色の科学	神戸大学高大連携特別講義(公開授業)	2017.7.27	神戸大学
河本敏郎	今高校生に求められる力とは～大学側から	日本物理教育学会近畿支部第 26 回物理教育を考える会 Part II	2017.10.14	京都教育大学
河本敏郎	光と色の科学	理学部模擬授業	2017.10.18	神戸大学
佐藤春実	テラヘルツ分光を利用した高分子の高次構造	第 4 回 関西接着ワークショップ	2018.1.25	大阪市立大学梅田サテライト 文化交流センター

Awards **受賞**

氏名	受賞研究題目	賞名	団体、学会名
黒田真司	単一モード紫外レーザーによるフルオレンの高分解能分光	優秀講演賞	第 17 回分子分光研究会
山本雄大	Time-Resolved EPR Study on Photoinduced Charge-Transfer Trap State in Thiophene-Thiazolothiazole Copolymer Film	2017 年光化学討論会 優秀学生発表賞（ポスター）	光化学協会
江間文俊	時間分解 EPR 法による室温リン光発光性有機包接結晶の励起三重項状態の電子構造	最優秀ポスター発表賞（CSJ 化学フェスタ賞）	化学フェスタ実行委員会
濱田実里	アフリカツメガエル由来クリプトクロムに生成する光電荷分離状態の電子的相互作用	第 56 回電子スピンサイエンス学会年会(SEST2017) 優秀ポスター賞	電子スピンサイエンス学会
狩俣出	Slow charge transfer process over a few nanoseconds in heterostructured $CH_3NH_3PbBr_{3-x}I_x$	2017 年光化学討論会 最優秀学生発表賞（ポスター）	光化学協会
櫻井学	光誘起電子移動反応における磁場効果を利用した新規蛍光イメージング法の開発	第 56 回電子スピンサイエンス学会年会(SEST2017) 優秀ポスター賞	電子スピンサイエンス学会
舟木千尋	テラヘルツ分光法によるポリカプロラクトンの紫外線劣化と高次構造の相関	エクセレントポスター賞	第 63 回高分子研究発表会（神戸）
岡本翔	In-plane magnetic anisotropy of hemin revealed by high-field and high-frequency electron spin resonance	2017 Springer Poster Award	5th Awaji International Workshop on "Electron Spin Science & Technology: Biological and Materials Science Oriented Applications"
岡本翔	強磁場・テラヘルツ領域におけるヘミンの精密 ESR 分光	優秀発表賞	電子スピンサイエンス学会
大木瑛登	圧力下強磁場 ESR による三角格子反強磁性体 $CsCuCl_3$ の研究	最優秀発表賞	修士論文審査会（2018 年 3 月）
堀江秀和	カシミール効果における静電気力補正	最優秀発表賞	修士論文審査会（2018 年 3 月）

Conference Organization 学術集会の開催

氏名	学術集会	共同主催者	場所	時期	参加者概数
富永圭介 (日本側代表)	10th Asian Conference on Ultrafast Phenomena	David Lee Phillips (the University of Hong Kong)	the University of Hong Kong, Hong Kong	2018.1.7-10	約 70 名
小堀康博	Kobe mini-symposium on exciton and charge dynamics		理学研究科 Z201・202 教室	2017.11.7	約 50 名

10th Asian Conference on Ultrafast Phenomena

Seminars セミナー

Date	Name	Affiliation	Title
8.4.2017	池田 浩	大阪府立大学大学院工学研究科	有機電子移動反応で実現する面白いこと：一電子σ結合と熱ルミネッセンスにみる電子移動反応の制御
9.25.2017	Amalendu Chandra	Indian Institute of Technology Kanpur	Dynamics of water and aqueous solutions from ab initio molecular dynamics simulations
1.18.2018	神取 秀樹	名古屋工業大学工学研究科	ロドプシンの生物物理学

Molecular Photoscience Research Center
Kobe University,
Nada, Kobe 657-8501 Japan

Tel: +81-78-803-5761
URL: http://www.research.kobe-u.ac.jp/mprc/about/index_e.html (English)

〒657-8501
神戸市灘区六甲台町 1－1
神戸大学分子フォトサイエンス研究センター

電話番号　078-803-5761
http://www.research.kobe-u.ac.jp/mprc/index.html（日本語）